Spring 5-15-2021

TARGETED COMBINATION THERAPY OF NSCLC USING TAXOL AND FINGOLIMOD LOADED NANOCERIA

Raghunath Narayanam
Pittsburg State University, rnarayanam@gus.pittstate.edu

TARGETED COMBINATION THERAPY OF NSCLC USING TAXOL AND FINGOLIMOD LOADED NANOCERIA

A Thesis Submitted to the Graduate School
in Partial Fulfillment of the Requirements
for the Degree of
Master of Science in Polymer Chemistry

Raghunath Narayanam

Pittsburg State University

Pittsburg, Kansas

May 2021

TARGETED COMBINATION THERAPY OF NSCLC USING TAXOL AND FINGOLIMOD LOADED NANOCERIA

Raghunath Narayanam

APPROVED:

Thesis Advisor _____
Dr. Santimukul Santra, Department of Chemistry

Committee Member _____
Dr. James McAfee, Department of Chemistry

Committee Member _____
Dr. Serif Uran, Department of Physics

ACKNOWLEDGMENTS

Firstly, I want to thank Dr Santimukul Santra for providing an opportunity to conduct research in his lab and designing me a project for thesis which matches my area of interest. His esteem knowledge and guidance helped me in every step throughout my entire research expertise.

I want to express my gratitude towards the chemistry department for providing all the support and encouragement during my study period in the university.

My special thanks to Dr Tuhina for your valuable help and guidance in the research. I want to thank all my fellow 'Nanotheranostics lab' members, especially Ruby for providing help directly or indirectly in various experiments.

Finally, a heartful thanks for my parents for providing me valuable education and my sister for her boundless support. I also want to thank my friends Prasanna, Vivek and Ramji for always being there for me.

TARGETED COMBINATION THERAPY OF NSCLC USING TAXOL AND FINGOLIMOD LOADED NANOCERIA

An Abstract of the Thesis by
Raghunath Narayanam

Among various types of cancers, lung cancer reports highest death rate and non-small cell lung cancer causes highest mortality in lung cancers. This is mainly due to the scarcity of treatment options and available treatments show numerous adverse effects. In recent times, nanotechnology paved a new path for the diagnosis and therapy of cancer. In this study, we worked on a novel, multifunctional nanoceria (NC) platform loaded with two unique drugs taxol and fingolimod, which acts in their own ways providing a synergic therapeutic effect. We hypothesized that the usage of the polyacrylic acid (PAA) coated nanoceria (PNC) increases the therapeutic efficacy of drugs and minimize the side effects. Nanoceria itself possess excellent Redox property and anti-tumor activity. Using 'click' chemistry the surface carboxylic groups of nanoceria are conjugated with the folic acid, which targets the folic acid receptor that is overexpressed in lung cancer A549 cells. We studied the cell death in a time dependent and dose dependent manner. The therapeutic effect of the nanomedicine was assessed with the help of ROS, cytotoxicity, apoptosis and migration assays.

TABLE OF CONTENTS

CHAPTER **PAGE**

LIST OF FIGURES

Chapter I

Chapter II

LIST OF ABBREVIATIONS

NC:	Nanoceria
PAA:	Polyacrylic acid
PNC:	PAA coated nanoceria
FNC:	Folate conjugated nanoceria
Tax:	Taxol
Fingo:	Fingolimod
EDC:	1-ethyl-3-(3-dimethylaminopropyl) carbodiimide
NHS:	N-hydroxy succinimide
DMSO:	Dimethyl sulfoxide
MTT:	(3-(4, 5-dimethyl-thiazol-2-yl)-2, 5 diphenyl tetrazolium bromide)
PBS:	Phosphate buffer saline
FBS:	Fetal bovine serum
DAPI:	4′,6-diamidino-2-phenylindole
MRI:	Magnetic resonance imaging
DLS:	Dynamic light scattering
DHE:	Dihydroethidium
EDA:	Ethylenediamine
ROS:	Reactive oxygen species

Chapter I

Introduction

Cancer, an abnormal growth of tissue at a specific or different part of the body, is now considered as one of the leading causes of death globally, which is responsible for approximately 10 million deaths per annum[1]. According to the World Health Organization, one in every six deaths is due to cancer.[2] Though some of the cancer tumors are benign, the malignant tumors possess the ability of rapid growth and invade other parts of the body and attack vital organs. This results in the metastasis, which is the reason for numerous deaths.[3] The growth in the number of cases is nowhere to be reduced in the near future due to the rapid escalation of risk factors in the various carcinogenic agents, such as physical (UV radiation), chemical (pollution, tobacco smoke, contamination of food and water) and biological (infections from several bacteria and viruses). In addition to this, lifestyle changes in the humans also lead to the cancer growth.[4,5]

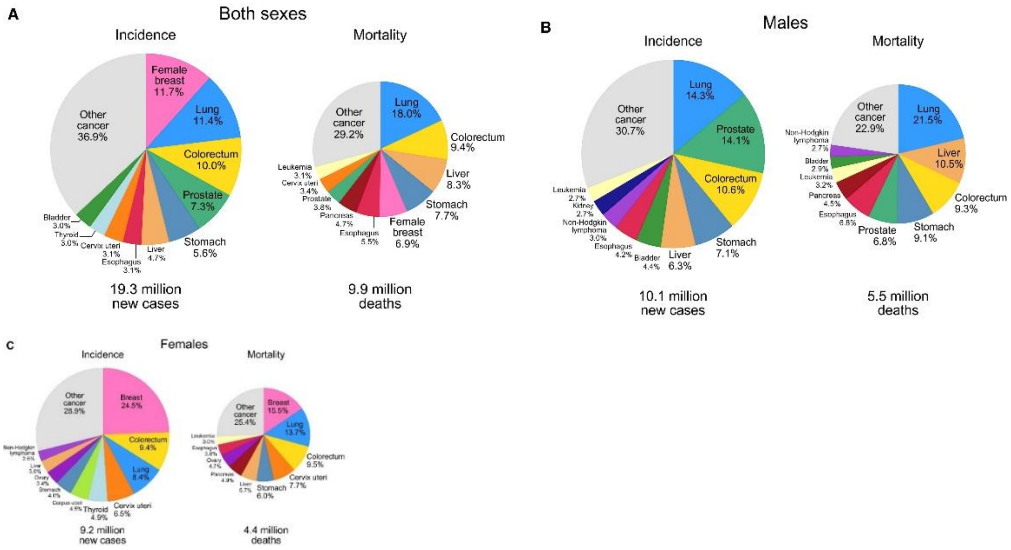

Figure 1. Distribution of Cases and Deaths for the Top 10 Most Common Cancers in 2020 for (A) Both Sexes, (B) Men, and (C) Women.**[3]**

Cancer is classified into different types, based on which organ is affects. The major type of cancers among these are: lung, breast, intestinal, prostate, skin, stomach, liver and thyroid.[6] As seen in **Figure 1**, lung cancer accounts for more deaths in males, whereas breast cancer has greater incidence rate and mortality rate in females.[7] In this research, we primarily focused on the treatment for lung cancer. Lung cancer is second only to breast cancer with regard to mortality rates and is the cause of 1.8 million deaths a year globally.[8] Lung cancer is primarily observed in smokers and even non-smokers are at an huge risk, due to the environmental carcinogens.[9] Other risk factors for lung cancer are genetics (patients with family history), radiation and asbestos.[10] There are two types of lung cancers: small cell lung cancer (SCLC) and non-small cell lung cancer (NSCLC).[11] **(Figure 2)**. Of these, NSCLC is a slow growing cancer and it does not develop any kind of symptoms until it is in advanced stage, resulting in the delay of treatment. NSCLC causes nine out of ten deaths by lung cancer, whereas SCLC is a rapidly growing type, comprising only 15 percent of total lung cancer cases.[12] Adenocarcinoma is the subtype of NSCLC, which accounts for up to 40 percent of the NSCLC.[13] For the diagnosis of lung cancer, oncologists generally use methods such as bone marrow aspiration and biopsy, computed tomography (CT) scan, magnetic resonance imaging (MRI), positron emission tomography (PET) scan, chest X-ray and pulmonary function tests.[14,15]

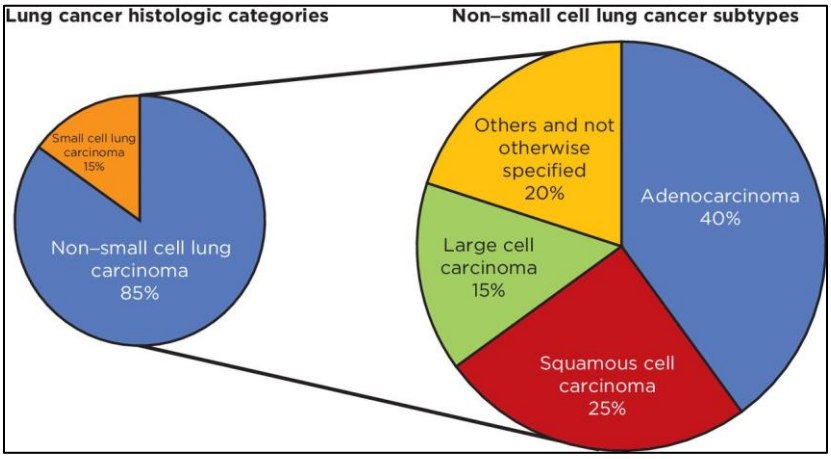

Figure 2. Histological classification of lung cancer and sub-types of NSCLC.[11]

Treatment of cancer:

There are various treatment options for lung cancer such as

a) **Surgery:** This process removes the tumor from organs through surgical procedures. Even after the surgery, there may be some trace amount of tumor cells that cannot be removed, which may undergo metastasis and develop into tumors.[16]

b) **Radiation Therapy:** This is a local therapy, in which tumors are exposed to X-rays and gamma rays, which damages the cancer cells.[17]

c) **Chemotherapy:** This is a widely used treatment option for lung cancers. In this method, anti-cancer drugs are administered in several doses through intravenous route. Commonly used chemotherapeutic drugs are paclitaxel, doxorubicin, cis-platin and others.[18,19] Despite its advantages, this procedure brings numerous side effects such as severe hair loss, fatigue, anemia and bleeding due to the lack of targeted delivery of the drug. Moreover, NSCLC becomes non-responsive to the conventional chemotherapy, due to the non-specific accumulation of the drugs, which leads to multidrug resistance (MDR).[20-22]

To minimize these side effects, many alternative therapeutic procedures are in place including immunotherapy, nanomedicine-based targeted therapy and the use of activatable prodrugs for the effective treatments. Activatable prodrug is a modified form of therapeutic drug that gets activated only inside the tumorous microenvironment under specific conditions.[23-24]

1) Nanomedicine:

Nanomedicine is one of the alternative therapeutics, which has shown promising results in recent years. It is the combination of nanotechnology, therapeutics, diagnosis and chemical biology.[25] The basic concept of this alternative therapy is to conjugate or encapsulate the desired therapeutic agent in higher dosage and deliver specifically to the tumor.[26] The main advantage of this innovative method is its targeting mechanism where surface was modified with receptor targeting molecules.[27] In addition, this nanomedicine approach brings diagnosis modality by incorporating various imaging agents for the real-time monitoring of the treatment using MRI, PET, computed tomography and other methods.[28] Nanomedicine is successful not only for its target specificity, but also for its clearance from the body. Because of its low size, it is easily cleared by kidneys and retention time is higher in blood circulation, which results in effective delivery to the tumor.[29] There are several types of nanoparticle systems used in the field of nanomedicine such as polymeric nanoparticles and metallic nanoparticles.[30]

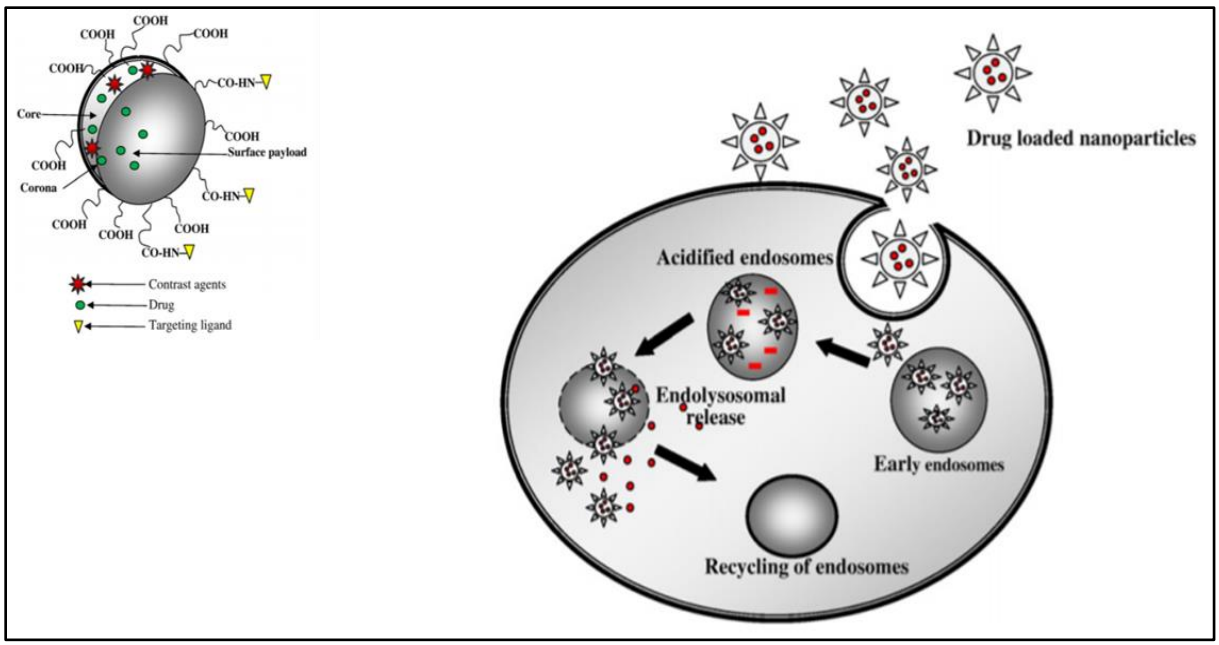

Figure 3. Schematic representation of cellular internalization mechanisms of Nanotheranostics.[32]

1.1) Polymer based nanoparticles for drug delivery:

The biocompatible and biodegradable polymers are used for the formulation of nanomedicines that can accommodate a wide range of therapeutic drugs and variety of imaging agents within its nanocavities.[31] Most polymeric nano capsules are made of hydrophobic core and a large number of polar reactive surface group. The core is used for accommodating the hydrophobic drug cargo, whereas the hydrophilic surface functional groups are mainly used for target specificity.[32,33]

a) Polymeric nanoparticles: During the past decade, the drug delivery system through polymeric nanoparticles has grown exponentially. The main reason behind this is due to the tunable size, stability and excellent biocompatibility and biodegradability.[34] Several linear polymers such as polyacrylic acid (PAA), polylactide-glycolic acid (PLGA) and polylactic acid (PLA) are used for the formulation of nanomedicines.[35] Sahoo et. al. has developed PLGA based nanoparticles for the cancer therapy, which extravasate through the tumor vasculature and deliver the drugs payload into the cells by enhanced permeability and retention (EPR) effect and increases the therapeutic efficacy, which accumulates more nanomedicine in the tumor, compared to normal tissues.[36] In general, the bioavailability of ocular drugs is less than 1 percent. To improve this, Aqil et. al. has developed a PLGA nanoparticle system for ophthalmic delivery, in which they encapsulated the drug sparfloxacin. This enhanced the bioavailability of the drug by increasing corneal penetration and prolonging precorneal drug residence time, compared to the free drug.[37] Pannala et. al. has synthesized a nanoparticle drug delivery system with the polymer poly lactic acid (PLA) and co-

encapsulating the drugs theophylline and budesonide for the lung diseases such as asthma and chronic obstructive pulmonary disease (COPD).[38] **(Figure 4)**.

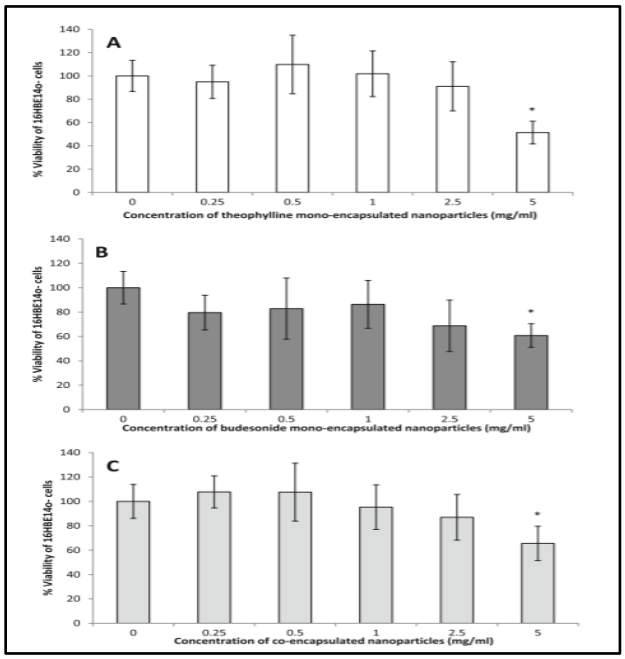

Figure 4. The effect of theophylline mono-encapsulated nanoparticles (A), Budesonide mono-encapsulated nanoparticles (B) Theophylline and budesonide co encapsulated nanoparticles (C) on the percentage viability of 16HE14o-cells.[38]

b) Polymeric micelles: Polymeric micelles are amalgamation of hydrophobic polymer cores and hydrophilic polymer chains. These are made from various copolymers. The hydrophobicity of the core protects the encapsulated drugs and dyes from undesired interactions and the hydrophilic outer shell makes the nanoparticles dissolve in water.[39,40] Matsumara et. al. has constructed polymeric micelles with block copolymers of polyethylene glycol (PEG) and polyaspartate and encapsulated them with various anticancer drugs such as paclitaxel, cisplatin and SN-38 individually and evaluated the efficacy through pre-clinical studies using mice.[41] These polymeric micelles have also been studied as cutaneous drug delivery system by Chavoshy et. al. for psoriasis. They have engineered the drug for a sustained release of anti-fungal drugs such as cyclosporin and ketoconazole.[42]

c) Dendrimers: Dendrimers are a major part of macromolecular architectural structures. They are three dimensional, perfectly branched and symmetrical. It consists of a core molecule and the exterior is highly functional, which can be modified by using various chemistries for attaching targeting ligands and groups which improves stability for various microenvironments.[43,44] Due to

the symmetric structure, dendrimers have a greater number of cavities, which can accommodate huge load of desired cargos.[45] Poly (amidoamine) or PAMAM is one of the widely used dendrimer for the drug delivery. Pokorski et. al. has developed a PEGylated dendrimer drug delivery vehicle to carry the drug Silicon phthalocyanine (Pc4) a photosensitizer used for treating fungal infections caused by *Candida albicans.* Even though the free drug is effective, its hydrophobicity limits the delivery. Hence, they used the dendrimer as a vehicle for better delivery and obtained good results.[46] Santra et. al. has recently developed a hyperbranched polyester using proprietary AB_2 monomer and diethylene glycol in a single step. This dendrimer was further used as a nano-carrier for the drug doxorubicin as a treatment for lung cancer. The surface of the dendrimer has been modified by conjugating folic acid for the better internalization into the cancer cells.[47] **(Figure 5)**.

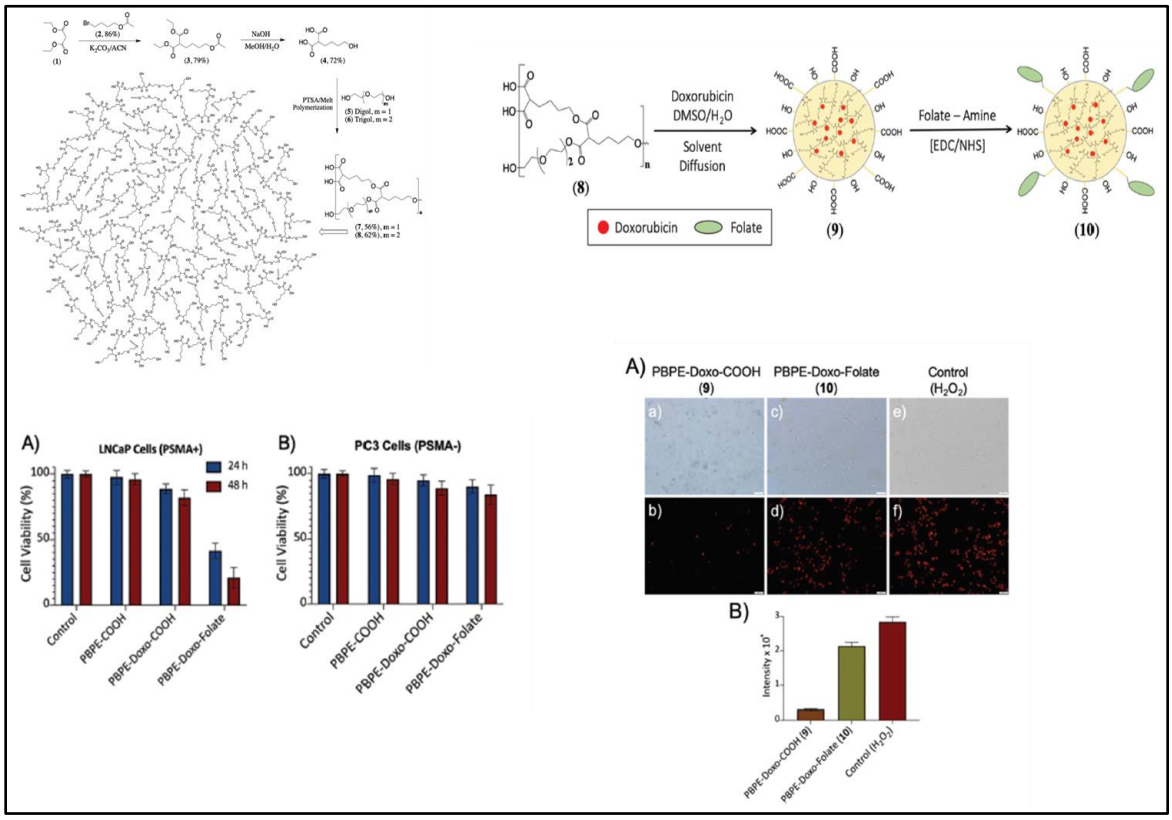

Figure 5. Schematic representation of the synthesis of PBPE dendrimer nanoparticle, encapsulation of cargo and surface modification of dendrimer, Determination of cytotoxicity and ROS in the cancer cells generated by nanomedicine. Nanomedicine with folate on the surface shows high toxicity compared to the other.[47]

1.2) Metal based nanoparticles: Various types of metallic nanoparticles which can be used for the drug delivery are Nanoceria (NC), Iron oxide nanoparticles (IONPs), Gadolinium nanoparticles (GdNPs) Quantum dots (QDs), gold nanoparticles (AuNPs), and carbon nanotubes (CNTs).[48,49] These can be used as drug delivery systems by coating the nanoparticles with a biocompatible polymer, which can be further modified. The motive behind the usage of the metallic nanoparticles is presence of some unique properties of these metals, which cannot be replicated by the polymers, such as MRI contrast imaging by iron oxide nanoparticles, antioxidant properties of nanoceria, better optical properties of gold nanoparticles, anti-bacterial property of the silver nanoparticles and distinctive catalytic properties of platinum nanoparticles.[50,51]

a) Iron oxide nanoparticles: Among all the metallic nanoparticles, IONPs are the most explored nanoparticles with diverse applications. These consist of magnetite core (Fe_3O_4) at the center and can be coated with a variety of polymers. They are superparamagnetic nanoparticles with dual imaging and therapeutic capabilities. Along with the drug delivering capabilities, IONPs are also used as a dark contrast imaging agent which allow to monitor the drug delivery using MRI machine.[52] Not only MR imaging, but also optical imaging can be achieved through incorporating several dyes in the polymer coating. Hence, IONPs can be used for multimodal (magnetic and fluorescent) and multifunctional (therapeutic and imaging) purposes. Desired cargoes can be encapsulated efficiently in the nanoparticles using solvent diffusion method.[53] Yang et.al. has explored the utilization of IONPs for the drug delivery along with MRI monitored magnetic targeting of brain tumors through in-vivo studies. Image analysis of their study revealed that magnetic targeting induced a 5-fold increase in the total glioma exposure to magnetic nanoparticles over non-targeted tumors and a 3.6-fold enhancement in the target selectivity index of nanoparticle accumulation in glioma over the normal brain. This indicates the enhanced drug delivery through IONPs can be achieved.[54]

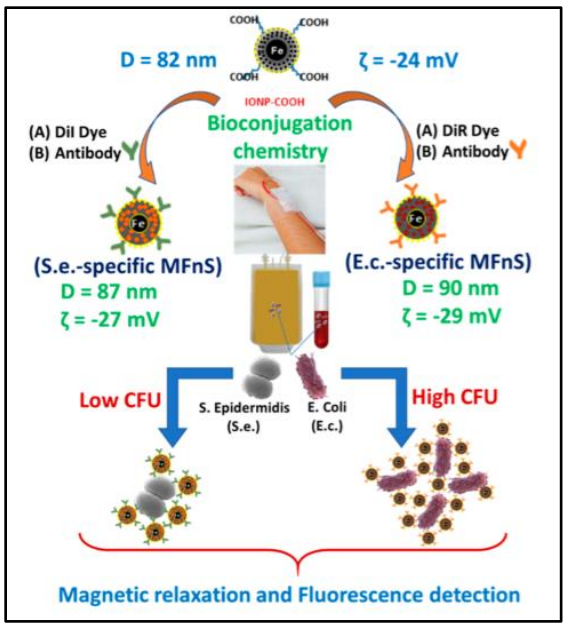

Figure 6. Schematic representation of the mechanism of dual-mode detection of bacterial contamination in whole blood and PCs using functional MFnSs.[55]

Santra et. al. has reported a design and synthesis of dual-modal magneto-fluorescent nano sensor (MFnS) by integrating magnetic relaxation and fluorescence modalities for the wide-range detection of blood-borne pathogens. MFnSs are designed to specifically detect *Staphylococcus epidermidis* and *Escherichia coli*, two of the predominant bacterial contaminants in blood and platelet concentrates. Specific interaction between the target pathogen and functional MFnS detects the colony forming units of bacteria. This nano sensor also discriminates between the pathogenic bacteria including *E. coli and S. epidermidis.* This nanotechnology helps in the early detection of pathogens and helping in therapy.[55] **(Figure 6,7)**

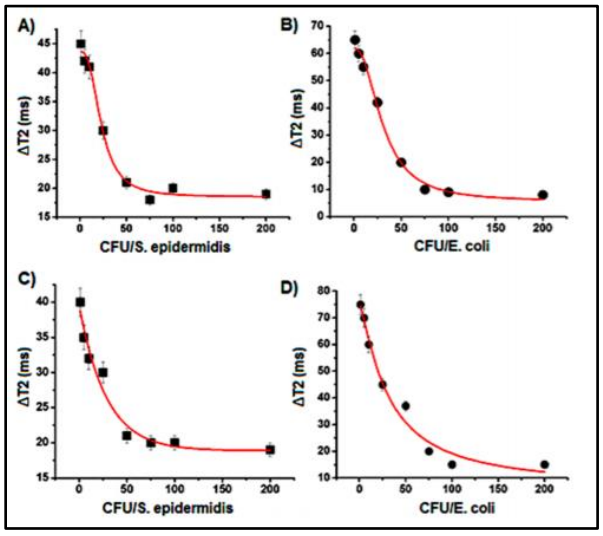

Figure 7. (A and C) S. epidermidis and (B and D) E. coli cultured in nutrient broth. Specific Ab-MFnS (200 µL, [Fe] = 2 mmol) was added to serially diluted samples (500 µL) of S. epidermidis or E. coli, each containing 200 µL of blood (A and B) and PC (C and D). After 15 min of incubation at 37 °C, the samples were transferred to a relaxometer tube, and T2 MR measurements were performed.[55]

b) Gold nanoparticles: These are one of the extensively used nanoparticles for the drug delivery because of properties such as inertness, biocompatibility, low toxicity and a standout feature known as surface plasmon resonance (SPR).[56] Gold nanoparticles are classified into various types based on their shape, such as nanosphere, nanorods, nanoshell, nanocage and nanostar.[57] **(Figure 8)**

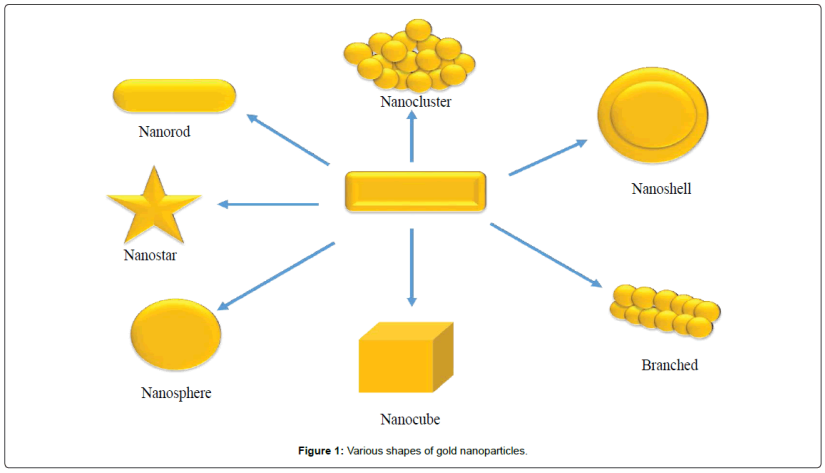

Figure 8. Different shapes of gold nanoparticles used for various biological applications.[57]

Wong et. al. has demonstrated the delivery of drug doxorubicin by Pegylated gold nanoparticles to the cancer cells. They modified the surface of nanoparticles by conjugating with folic acid for better internalization. They evaluated the cytotoxicity in both drug sensitive liver cells (HepG2) and drug resistant liver cells (HepG2-R) and the internalization of free drug is minimal in the drug resistant cells, whereas it is more with the drug-gold nanoparticle complex.[58] Haick et. al. has developed a sensor based on the gold nanoparticle to detect the presence of lung cancer through exhaled breath. Contrary to the conventional diagnostics, the use of this nanosensor is viable and efficient. This nanosensor works by the combination of solid phase microextraction and gas chromatography, which can detect up to 42 volatile organic compounds that represents the cancer biomarkers.[59]

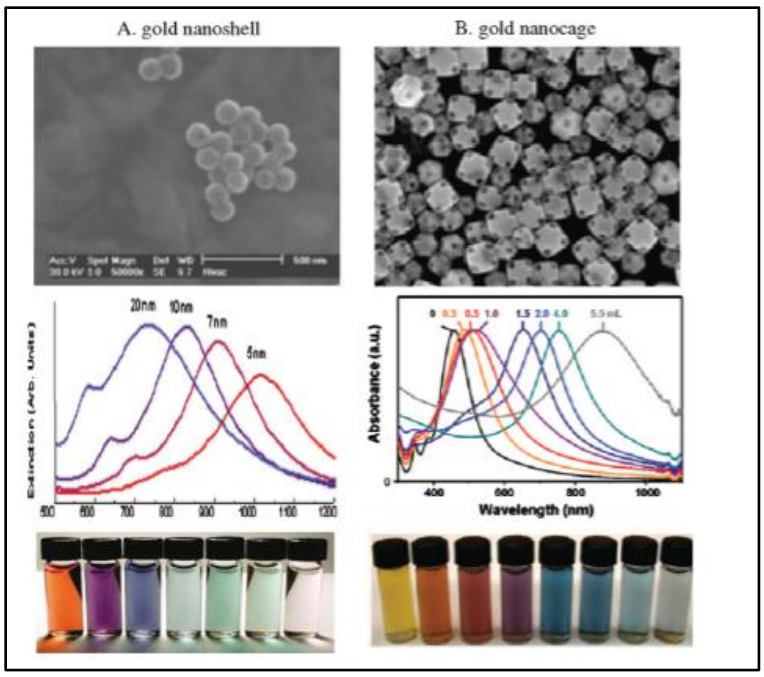

Figure 9. Tunable optical properties of gold nanoshells by changing the shell thickness (A) and gold nanocages by changing the auric acid in the synthetic procedure (B). Top row: TEM; middle row: absorption spectra.[60]

By using the optical and photothermal properties of plasmonic nanoparticles, El-Sayed et. al. has addressed the applications of cancer imaging and the photothermal therapy in their research. They worked on both nanorods and nanocages of various sizes. They made significant improvements in imaging based on light scattering by dark field microscopy and done spectroscopic detection by inducing magnetic field and Raman spectroscopy. They also used the gold nanoparticles for photothermal therapy, in which photon energy is converted to heat sufficient to induce cellular damage via thermal effects such as hyperthermia, coagulation and evaporation.[60] **(Figure 9,10)**

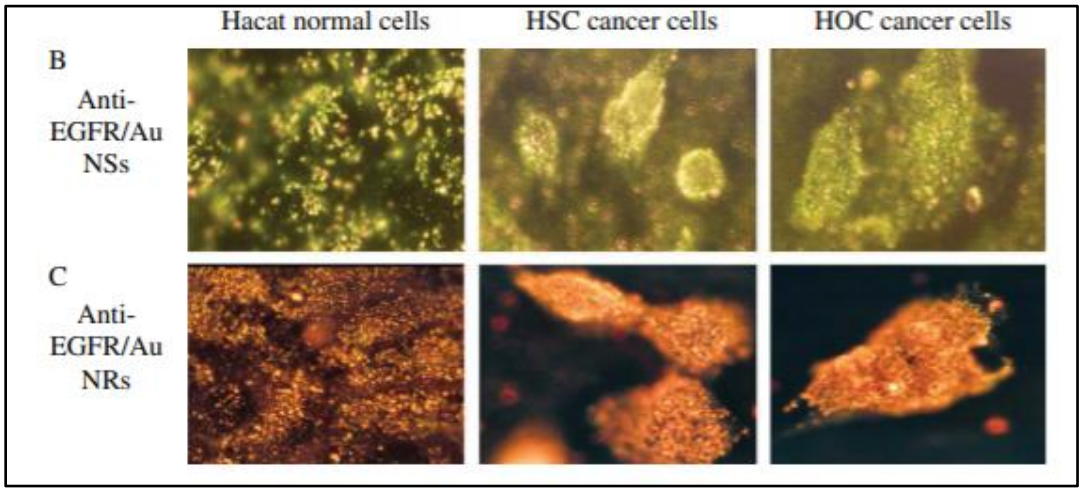

Figure 10. (B) Cancer cell diagnostics using dark field light scattering imaging of spherical gold nanoparticles; (C) Cancer cell diagnostics using dark field light scattering imaging of gold nanorods. The anti-EGFR-conjugated gold nanoparticles are bound to the cancer cells assembled in an organized fashion, while they are randomLy distributed around normal cells, thus allowing for the optical differentiation and detection of the cancer cells. While gold nanoparticles show color in green due to SPR in visible region and gold nanorods show color in red due to SPR in NIR region.[60]

c) Silica nanoparticles: Mesoporous silica nanoparticles (MSNs) are a variety of inorganic nanomaterials, which are largely used for biological applications for their large surface areas, tailorable pore sizes and multifunctional surfaces, both external and internal.[61] Tamanoi et. al. has tested the biocompatibility, biodistribution and drug delivery efficiency of MSNs using nude mice. They determined the maximum tolerated dose of MSNs in the mice. They concluded their study by determining that there is significant accumulation of MSNs in tumors, but not in the normal tissues, which proves that MSNs are promising vehicles for drug delivery.[62] Zhao et. al. has functionalized the MSNs surface with amino-β-cyclodextrin rings bridged by cleavable disulfide bonds. This helped in trapping the drugs inside mesopores and blocking their release, which can be only released by high concentration of glutathione present in the cytoplasm of cancer cells, which cleaves the disulfide bonds.[63]

Prasad et. al. reported a novel nanoformulation of a photosensitizer (PS) for photodynamic therapy (PDT) of cancer, where the PS molecules are covalently incorporated into organically modified MSNs. Contrary to the popular opinion, there are several studies that reported toxicity of silica nanoparticles in pre-clinical studies.[64] Hudson et al. reported that intraperitoneal or intravenous administration of 1.2 g kg^{-1} MSNs is lethal to SV129 mice but is safe when reduced to 40 mg kg^{-1}.[65] **(Figure 11)**

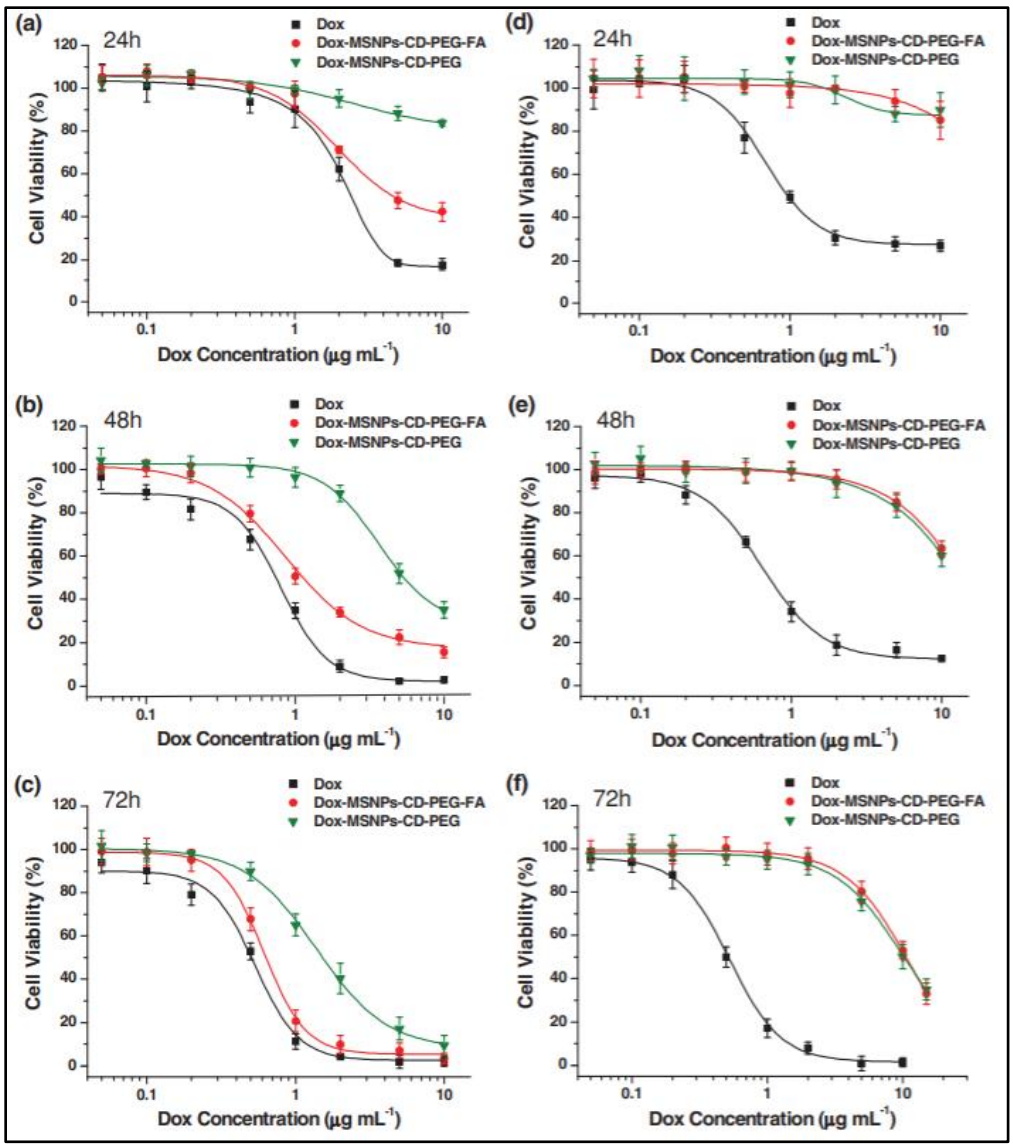

Figure 11. Cell Viability of HeLa cells (a,b,c) and 293 cells (d,e,f) incubated with free Dox, Dox-MSNPs-CD-PEG-FA and Dox-MSNPs-CD-PEG at different Dox doses. The cells were exposed to the samples for the indicated times.[65]

d) Silver nanoparticles: These are one of the oldest metallic particles used for the anti-bacterial applications. Nowadays, AgNPs are also being used as drug delivery systems because of the properties like plasmonic resonance and good biocompatibility.[66] Foldberg et. al. has synthesized Poly vinyl pyrrolidone (PVP) coated Ag nanoparticles and determined dose dependent cytotoxicity and gene toxicity by Ag^{+} ions in the human lung cell line of A549 cells through MTT assay and ROS stress.[67] Kumar et. al. has enhanced the efficacy of antifungal drug Miconazole by encapsulating it with silver nanoparticles, which itself is a potential antifungal agent, which is

highly effective against certain *candida* strains.[68] Yuan et. al. investigated the synergic effect of AgNPs and anticancer drug Gemcitabine (GEM) in the human ovarian cancer cell line A2780. It is known that AgNPs possess a unique cytotoxic effect to induce apoptosis in variety of cancer cells. From the data obtained by various cytotoxicity assays and ROS assays, they determined that combined treatment of AgNPs and GEM has significantly higher toxicity in the A2780 cells, when compared with the individual treatment.[69] **(Figure 12,13)**

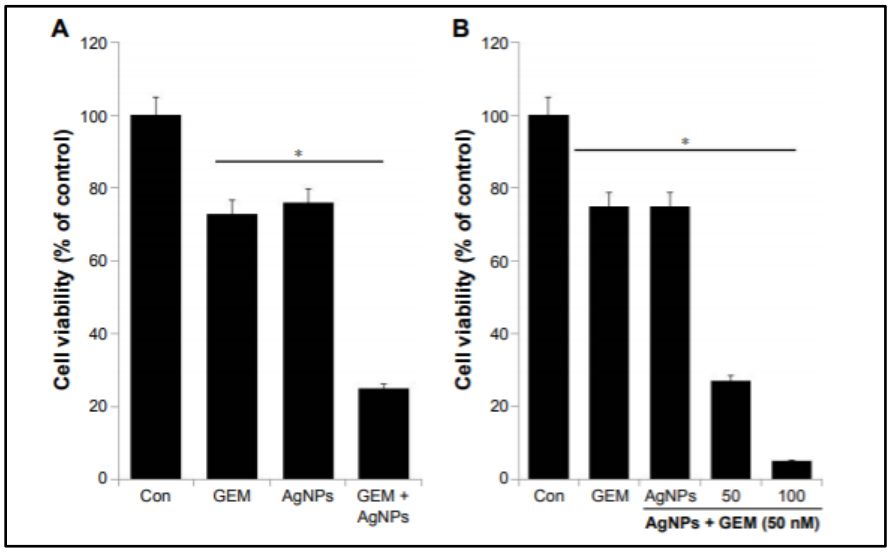

Figure 12. Cell viability assay determining the cytotoxicity of drug-nanoparticle combination. (A) A2780 were incubated with GEM (50 nM) and AgNPs (50 nM). (B) A2780 cells were incubated with a combination of different concentrations of AgNPs (50 and 100 nM) and a fixed concentration of GEM (50 nM) for 24 h.[69]

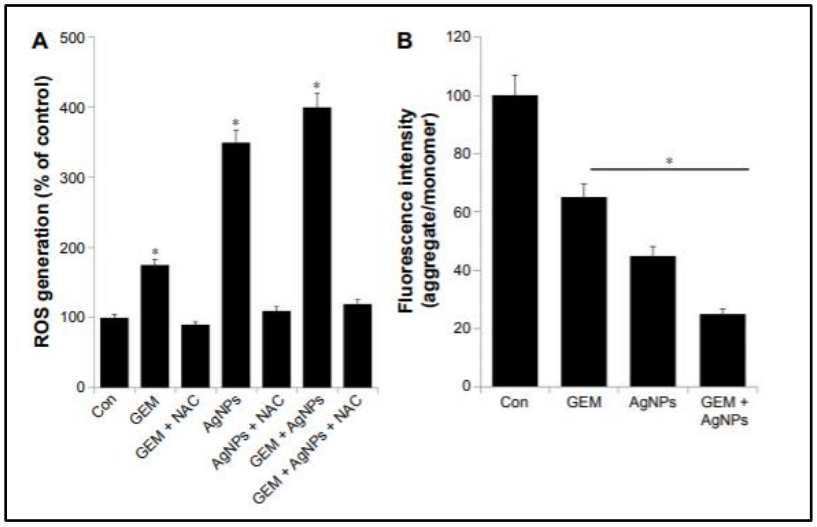

Figure 13. The effect of GEM, AgNPs, or a combination of GEM and AgNPs on oxidative stress in human ovarian cancer cells. (A) The levels of ROS were assessed by measuring the relative

fluorescence of 2′,7′-dichlorofluorescein using a spectrofluorometer. (B) Cells were treated with GEM (50 nM), AgNPs (50 nM), or the combination of GEM (50 nM) and AgNPs (50 nM) for 24 h; MMP (measured as a ratio of JC-1 aggregate to monomer) was determined after the treatments.[69]

e) Cerium oxide nanoparticles: Belonging to the lanthanide series, cerium is one of the abundant and rare earth metals available. Overtime, cerium oxide emerged as one of the important nanocarriers for drug delivery due to its advantages such as stronger reactivity, higher surface to volume ratio for better oxygen exchange and it also possess a unique property, that switches oxidation states between Ce^{3+} to Ce^{4+} which makes it a potential particle for redox state modulation, which is an important property for drug delivery.[70] According to the previous studies, cancer cells generate higher ROS when compared to normal stress. Nanoceria is extensively studied for its role as ROS scavenger in the therapy of cancer because of its antioxidant property.[71] Not only this, but also the antioxidant property is used in various biological studies including anti-inflammatory, anti-aging and oxidative stress related complications.[72] Various biological properties of nanoceria have been discussed in detail below:

Antioxidant activity: The ability of nanoceria to switch the oxidation states from Ce^{+3} to Ce^{+4} has been compared to that of biological antioxidants. Synthesis of the nanoceria in biocompatible media has been a challenging task and the process should not interfere with the redox capability of nanoparticles.[73] McGinnis et. al. has shown that the retinal degeneration which is induced by intracellular peroxide molecules can be prevented by nanoceria. These in-vivo investigations established the role of nanoceria in preventing vision loss due to light-induced degeneration of photoreceptor cells.[74] Korsvik et. al. has studied the interaction of nanoceria with ROS using superoxide dismutase (SOD) model, in which nanoceria competed with cytochrome-c for reduction by superoxide.[75] Patel et. al. has conducted experiments with human monocytic leukemia cells (THP-1) cells to evaluate free radical scavenging activity of nanoceria. They reported significant reduction of ROS in the species.[76]

Radio protective: Radiation therapy is one of the important treatments of cancer, in which gamma radiation is focused on the tumor sites. There are some harmful side effects for this procedure such as fatigue, swelling, neutropenia, nausea, dermatitis and damage to tissues around the tumor sites. To minimize these side effects, several radio protectors were introduced. Nanoceria exhibits excellent radio protectivity for the healthy tissues.[77] Tarnuzzer et. al. has engineered the cerium nanoparticles for protection from radiation induced cellular damage in the normal human breast cell lines. Both normal breast cells (CRL8798) and breast cancer cells (MCF-7) were cultured and treated with NC for 24h before exposing them to the radiation. After the radiation treatment, they

observed from the studies that nanoceria protected CRL8789 cells from the radiation, but not cancer cells (MCF-7). [71] Hosseinimehr et. al. has studied the radioprotective effect of nanoceria against genotoxicity induced by ionizing radiation on human lymphocytes. Normally, healthy lymphocytes when treated with IR, produces IL-1β in the microenvironment which leads to apoptosis and DNA damage. Here, they had treated the lymphocytes with nanoceria before exposing to ionizing radiation. This resulted in a 73% decrease of cell death when compared with untreated cells. This happened because nanoceria reduced IL-1β production, which restricted the cells to undergo apoptotic process.[78]

Radio Sensitizer: Main disadvantage for radiation therapy is the resistance developed by tumors overtime. There are several radio sensitizing drugs, such as suberoylanilide hydroxamic acid (SAHA). But there are several limitations including nausea, vomiting, dehydration and fatigue.[79] Contrary to the radioprotective property of nanoceria in the healthy cells, they also sensitize cancer cells to comply with radiation therapy. This effect is due to the reduction of ROS stress, which leads to the cell death.[80] Ghibelli et. al. has described the radio sensitization by nanoceria in HaCat keratinocytes. They observed that the cell death is occurring not due to the DNA damage by ionizing radiation, but by increasing efficiency of the cell perception to DNA damage, which further leads to the apoptosis of tumor cells.[81] Feng chen et. al. reported the radio sensitizing ability of nanoceria against breast cancer cell line. They encapsulated anti- cancer drug neogambogic acid in nanoceria. They treated the cells with three conditions including NGA-NC, only radiation and NGA-NC-IR. Of these, the combination of all the three shows more apoptotic cell death, when compared with the other two. This indicates the role of nanoceria in sensitizing cancer cells for the radiation therapy.[82]

1.4) Other nanoparticles: Apart from these, there are several other nanoparticles, which are biocompatible and useful for the drug delivery. In contrast to the iron oxide nanoparticles, which produce dark images, there are gadolinium nanoparticles that can be used as Bright contrast imaging agents, which produce bright images. These nanoparticles are often coated with the polymers with carboxyl or amine functional group on the surface, which are further used to conjugate with drugs and dyes for therapy and imaging.[83] Nowadays, research has been conducted on some biological nanoparticles such as viral nanoparticles. These nanoparticles have several advantages including availability at various sizes, biocompatibility, surface modification and non-virulency. Several plant viruses such as tobacco mosaic viruses are being bio-engineered into nanoparticles.[84]

Conclusion: By observing the statistics around the globe, cancer is considered as a leading cause of mortality and among various types of cancers, lung cancer is the most dangerous type. The main reason for high mortality of cancer is the lack of early diagnosis, since the symptoms may not be experienced by majority of the patients. Secondly, poor bioavailability of neoplastic drugs to the tumors and very few treatment options with lethal side effects has also made this disease difficult to get treated. To minimize the side effects, extensive research has been going on. Novel drug delivery through nanoparticles is one of such research. Among the nanomedicines, there are several types including polymeric and metallic nanoparticles. These nanoparticles are highly effective, biocompatible and target specific. Each of these nanoparticles have their unique method of approach towards the target. Not only as therapeutic agents, but they can also be used for diagnostic approaches. Through this novel drug delivery methods, treatment of cancer can be produced in an efficient way with minimal side effects.

Chapter II

Results and Discussions

Introduction

Cancer is one of the leading diseases, which has a high mortality rate globally. There has been a steep increase in the number of cases in recent times, mainly because of biological and internal factors, environmental factors, occupational risks and various lifestyle changes.[1] The most common types of cancers are lung, breast, prostate, skin and stomach.[6] Among these, lung cancer records the highest number of cases majorly due to high consumption of tobacco and exposure to environmental carcinogens.[9] There are two types of lung cancers, small cell lung cancer (SCLC) and non-small cell lung cancer (NSCLC). Nine out of ten lung cancer cases are related to NSCLC which is slow growing and metastatic, on the other hand, SCLC spreads rapidly inside the body.[11-13] There are various types of treatment options for lung cancer, such as surgery, radiation therapy, chemotherapy and hormone therapy.[16,17] Among those, chemotherapy is the widely used method for cancer treatment. In this method, anticancer drugs like paclitaxel and doxorubicin will be administered through intravenous or oral route.[18] Since target specificity is not present in these drugs, they affect healthy cells which lead to several adverse effects.[19] There are several alternative therapies to reduce the side effects. Nanomedicine is one of the alternative therapeutics, which evolved into a noteworthy technology in the field of medicine for its drug delivering capabilities. Availability of diverse biodegradable nanoparticles, better drug loading capabilities and facile surface modification for the target specificity made this alternative therapy, a predominant method for drug delivery.[23,24]

In this work, we studied drug delivery through Nanoceria. Cerium oxide is known to have diverse applications because of its Redox property. It is used as a therapeutic agent because of its anti-invasive, radio protective, radio sensitizing, oxidant-mediated apoptosis, and antiangiogenic properties.[71,72] In this study, Polyacrylic acid coated nanoceria was conjugated with folate amine, with folic acid on the surface by EDC/NHS chemistry. This helps the nanoparticle to attach to the folate receptors which are abundantly present on the tumor cells. Nowadays, a new type of dosage

regimen is being followed for cancer, in which a cocktail of drugs is given for effective treatment. The drugs used in this process should affect the cancer cells in different pathways. The main reason behind this strategy is to provide synergistic effect for the drugs, which increases the therapeutic efficacy.[84]

In our study, we encapsulated Folate-Nanoceria with the drugs Taxol and fingolimod. Taxol binds to tubulin, the protein component of microtubules and enhances the polymerization of tubulin, which stabilizes the microtubules. This drug also interacts directly with the microtubules and stabilizes them against depolymerization by calcium, which instantly depolymerizes normal microtubules.[85] Since taxol has a specific binding site on the microtubule, it works more effectively. Moreover, it is also reported that taxol blocks the cells in the G2/M phase of cell division, which results in the formation of defective cells, which are unable to form normal mitotic apparatus.[86]

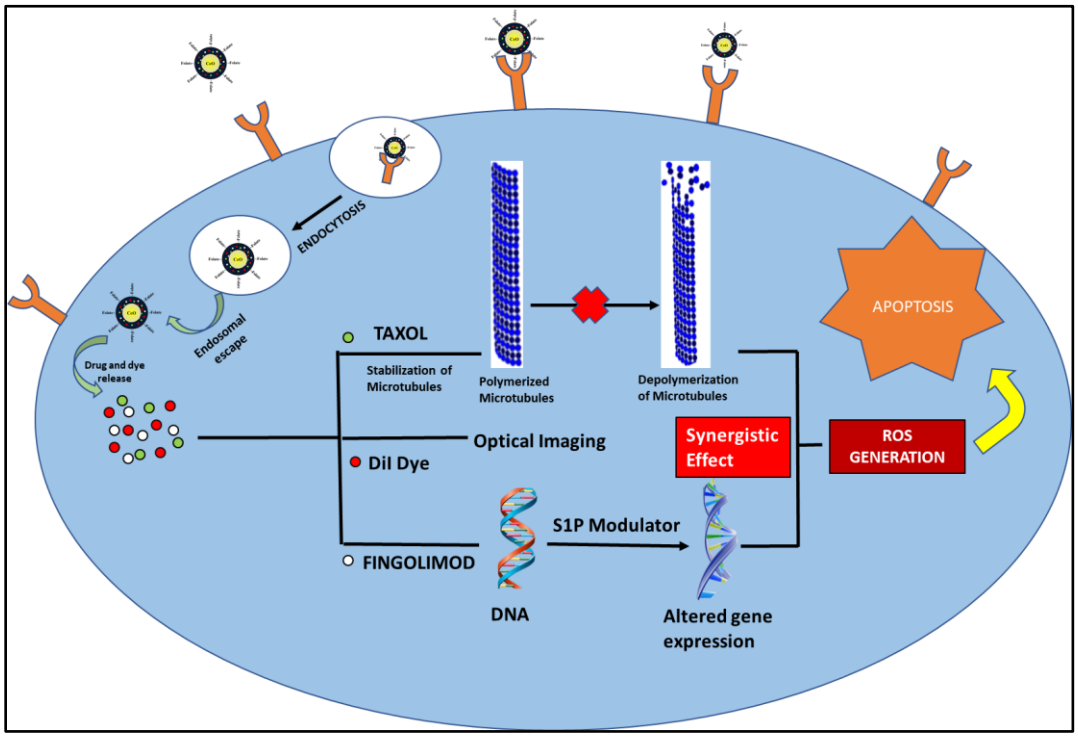

Figure 14. Schematic representation of the proposed mechanisms of the action of taxol and fingolimod for the treatment of NSCLC.

On the other hand, FTY70, which is generally known as fingolimod is sphingosine analogue and sphingosine-1-phosphate (S1P) receptor antagonist. This drug is clinically approved immunomodulating therapy for multiple sclerosis.[87] The mechanism of action of fingolimod changes according to the cancer cell line. In normal cells, the S1P signaling plays a major role in apoptosis. Only a few cancer cell lines reported apoptosis. In lung cancer cells, this drug helps in

the escape of cell death, which makes the cells more compliant to therapy.[88] We evaluated the effect of these drugs on the cell line A549, which are lung cancer cells. We also conjugated our nanoparticle complex with the DiI dye to monitor the efficacy of drugs through optical imaging.

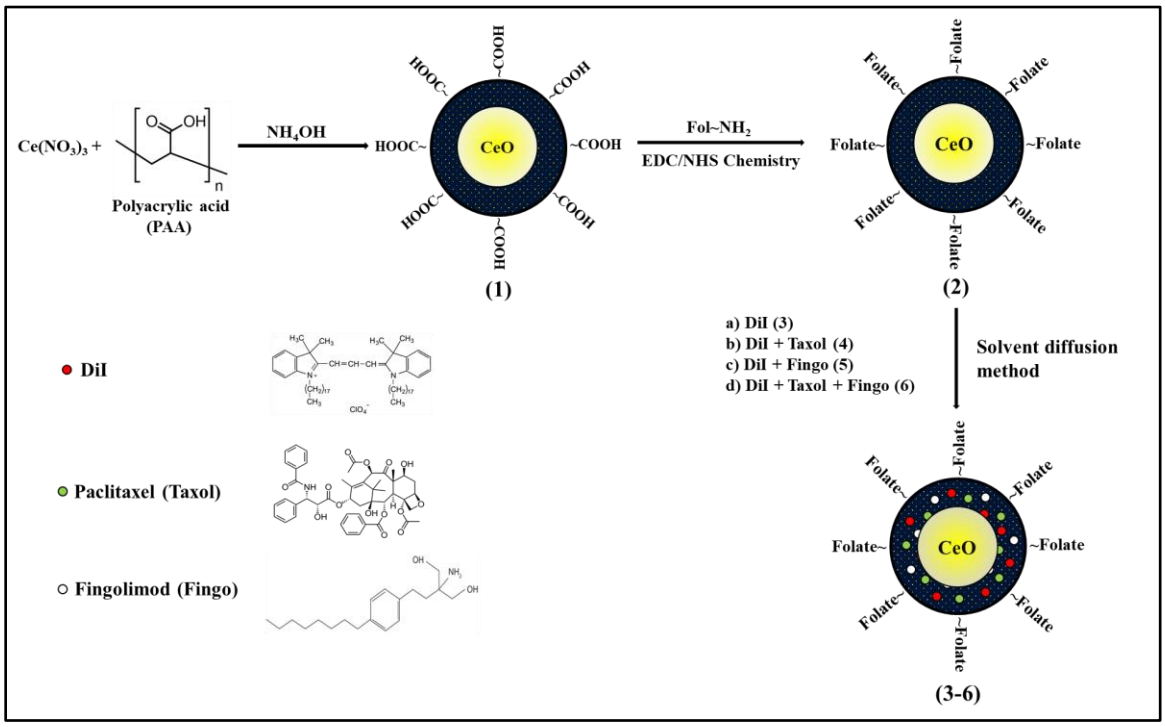

Scheme 1. Schematic representation of the synthesis of functional nanoceria. Polymer coated nanoceria **(1)** was synthesized using alkaline precipitation method. EDC/NHS chemistry was used to conjugate folic acid on the nanoceria and synthesize functional nanoceria **(2)**. Solvent diffusion method was used to encapsulate theranostics and dye inside the functional nanoceria **(3)**.

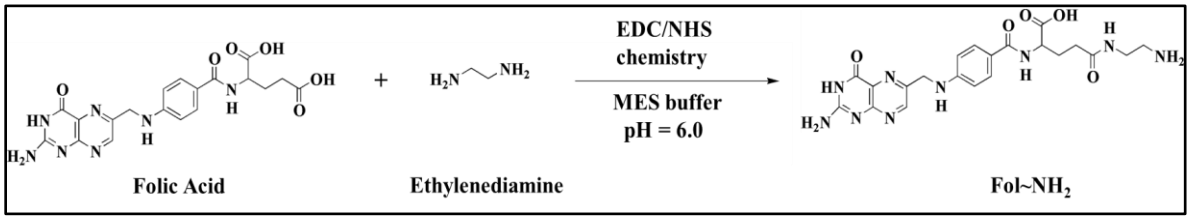

Scheme 2. Synthesis of folate-amine for the surface modification of cerium oxide nanoparticles.

2) Results and discussion:

2.1) Synthesis and characterization of functional cerium oxide nanoparticles

PAA coated nanoceria (PNC 1, **Scheme 1**) was synthesized using the solvent precipitation method, which was reported in the experimental section. The obtained yellow colored nanoceria was further centrifuged to reduce the particle size and eliminate any clusters or agglomerates present. The final nanoceria was further purified by dialysis technique, using a dialysis membrane (MWCO 6-8 KDa), which eliminates the unreacted starting materials like PAA and NH_4OH from the PNC. To this modified nanoceria, DiI dye was encapsulated using solvent diffusion method. The PAA coating on the NC makes it a stable nanoparticle for drug delivery and the carboxylic groups help to conjugate with various receptor molecules. The average size (diameter) and overall surface charge (zeta potential) which are measured using Dynamic Light Scattering (DLS) are 69 ± 2 nm (**Figure 15 A**) and -46.1 mV (**Figure 15 B**) respectively. This lipophilic encapsulated PNC was further used in the study as a negative control for optical imaging and to study the extent of internalization of PNC. In this study, we used the DiI dye as an imaging agent because of its high extinction coefficient ($\varepsilon > 125\ 000\ cm^{-1}\ M^{-1}$) and great fluorescence emission ($\lambda max = 565$ nm).

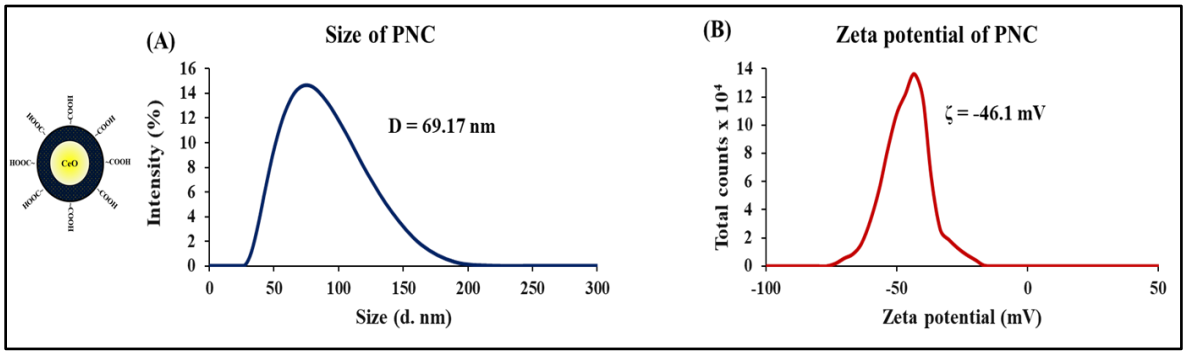

Figure 15. Dynamic light scattering (DLS) determined values of **(A)** Size of PNC and **(B)** zeta potential of PNC.

For nanoceria to be functional, i.e., to make the nanoceria enter the cytoplasm of the cancer cells, its surface was modified and conjugated with folic acid. For this process, PNC without the DiI was used. Folic acid was conjugated using EDC NHS chemistry. At first, structure folic acid was modified with ethylene diamine (EDA) (2 µL EDA in 100 µL DMSO) using EDC (5×10^{-3} moL) and NHS (3×10^{-3} moL) in the presence of MES buffer which results the synthesis of folate-amine (**Scheme 2**). This folate amine (250 µL) was bonded with PNC using EDC (5×10^{-3} moL) and NHS (3×10^{-3} moL) in the presence of MES buffer. The obtained folate conjugated nanoceria (FNC **2, Scheme 1**) was dialyzed for further purification. Then, DiI dye ($\lambda_{max} = 565$ nm) was encapsulated to FNC using solvent diffusion method as mentioned before, formulating DiI- encapsulated FNC, which was used as a positive control for optical imaging and monitoring treatment. Further, the

overall size and surface charge were determined as 72 ± 2 nm (**Figure 16 A**) and, -29.3 mV (**Figure 16 B**) respectively, using the DLS.

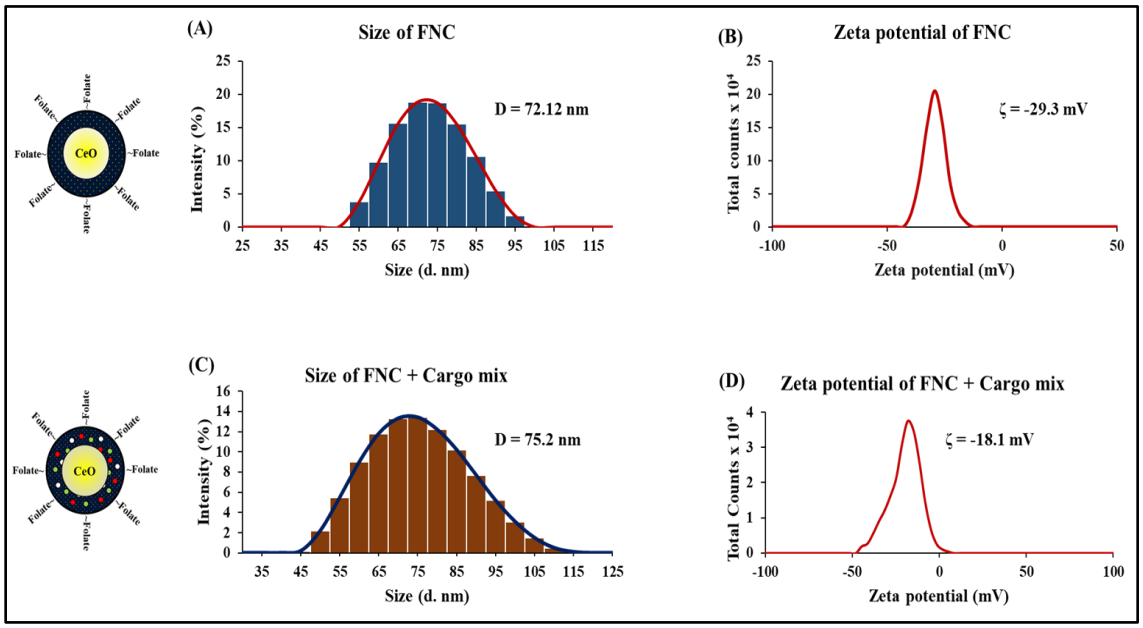

Figure 16. Overall size and surface charge of FNC and functionalized FNC characterized using Dynamic Light Scattering (DLS). **(A)** Size of FNC, **(B)** Zeta potential of FNC, **(C)** Size of FNC + Theranostics and **(D)** Zeta potential of FNC + theranostics.

The DiI dye labeled FNC was further used as a nanoprobe for the drug delivery into the folate overexpressing cancer cells. This FNC was encapsulated with drugs taxol (20 µL, 10 µg/µL) and fingolimod (4 µL, 10 µg/µL) using the solvent diffusion method. Finally, the drug and dye loaded functional nanoceria (**3, Scheme 1**) was purified with dialysis and stored at 4 ^{o}C for drug delivery studies. The overall diameter and the surface charge of the drug encapsulated functional nanoceria were 75 ± 2 nm (**Figure 16 C**) and -18.1 mV (**Figure 16 D**), respectively.

UV-vis and fluorescent experiments using a plate reader were done to determine the successful encapsulation of dye and drugs inside the PAA polymer. The absorbance spectrum of DiI encapsulated FNC confirmed the presence of both folic acid (λ_{max} = 352 nm, **Figure 17 A**) and DiI dye (λ_{max} = 568 nm, **Figure 17 B**). The fluorescence spectra of folic acid were found to be at λ_{max} = 564 nm (inset of **Figure 17 A**). Fluorescence spectra of functional FNC (**Figure 17 C**) further confirms the presence of both folic acid (λ_{max} = 447 nm) and DiI dye (λ_{max} = 574 nm). A comparative fluorescence study was done between the free DiI and encapsulated DiI, which are λ_{max} = 564 nm and λ_{max} = 572 nm (**Figure 17 D**), respectively.

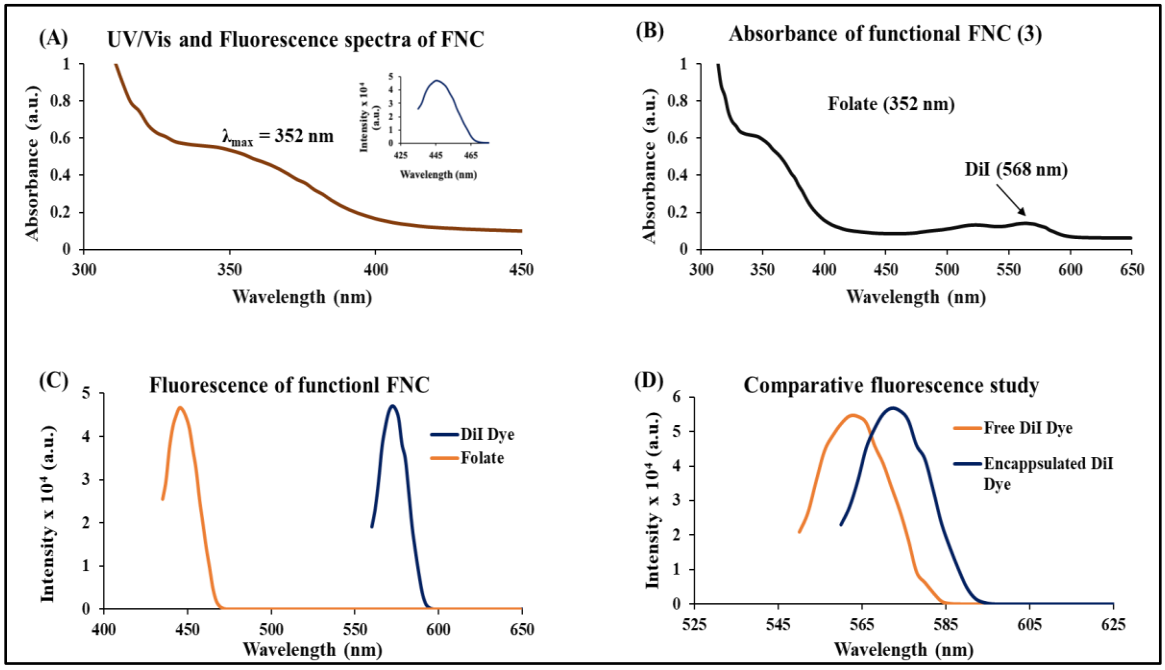

Figure 17. Characterization of FNC. **(A)** UV/Vis absorbance and fluorescence spectra of FNC, **(B)** Absorbance spectra of functional FNC, **(C)** Fluorescence spectra of functional FNC and **(D)** Comparative fluorescence spectra of free DiI and encapsulated DiI.

The presence of theranostics taxol and fingolimod were confirmed by the UV-vis spectrum with absorbance λ_{max} = 320 nm (**Figure 18 A**) and λ_{max} = 293 nm (**Figure 18 C**), respectively. The effective folate conjugation and the encapsulation of drugs and dye was further determined using the fluorescence spectrum. The fluorescence spectra of taxol and fingolimod are λ_{max} = 379 nm (**Figure 18 B**) and λ_{max} = 340 nm (**Figure 18 D**), respectively. The hydrodynamic size and fluorescence maxima of the nanoceria formulations remains unchanged for a long time. This indicates the stability of nanoparticles in the PBS buffer, which is equivalent to serum.

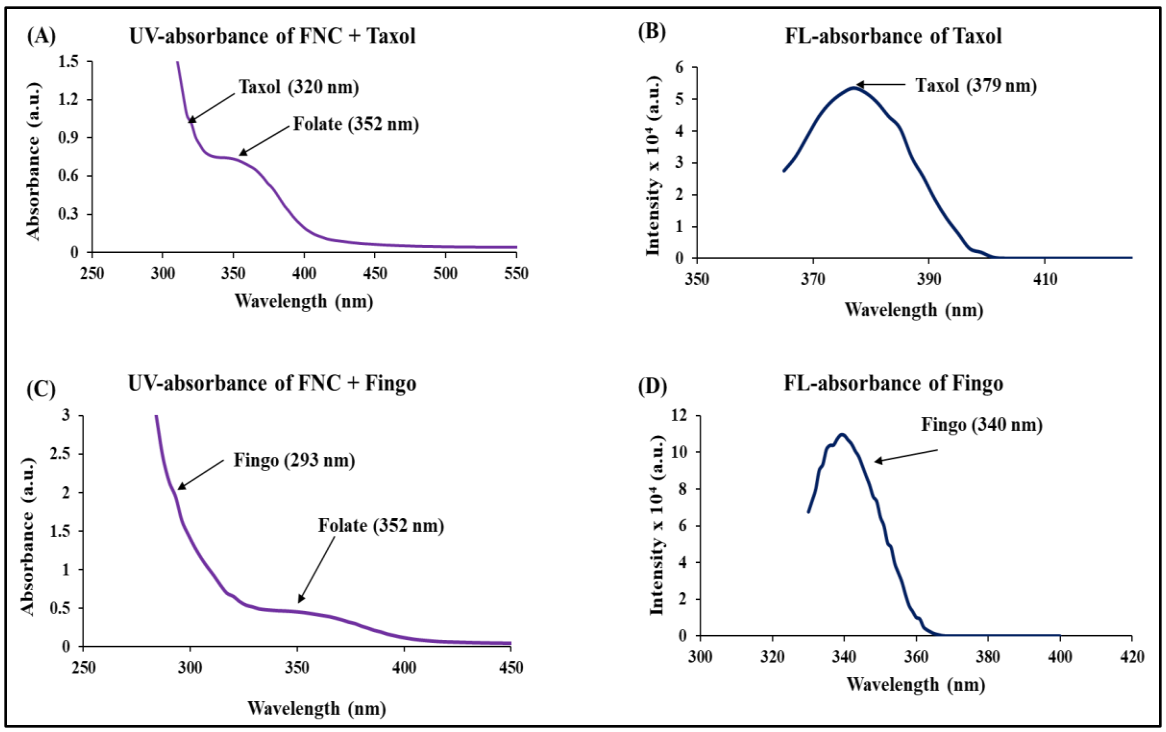

Figure 18. Characterization of FNC with theranostics. **(A)** Absorbance spectra of FNC-Taxol, **(B)** Fluorescence spectra of FNC-Taxol, **(C)** Absorbance spectra of FNC-Fingo, and **(D)** Fluorescence spectra of FNC-Fingo.

2.2) Cytotoxicity Studies:

After characterization, we studied the biocompatibility and evaluated cytotoxicity of theranostics loaded nanoceria using cell viability MTT assay. Cytotoxicity was determined using this assay by MTT, where live cells convert MTT into purple formazan crystals, which regulates mitochondrial activity. Absorbance of purple formazan crystals will be high in the presence of active living cells and low absorbance indicates less mitochondrial activity and more dead cells. This assay is generally used to study cytotoxicity of various drugs in different cell lines.

For this assay, we treated our nanoceria on lung cancer A549 cells (NSCLC, Folate receptor +) and VERO cells (Kidney epithelial cells, Folate receptor -). Cell viability was measured in A549 cells after treating with PNC, FNC, FNC-Taxol, FNC-Fingo and FNC-Taxol-Fingo in a single dose (40 µL, 2.0 mM) for 12 h, 24 h, 36 h and 48 h **(Figure 19)**. From the result, we observed that there is no cytotoxicity in the cells treated with PNC and FNC because of the absence of drugs. Among the drug loaded nanoparticles, Fingolimod showed less toxicity and combination of both taxol and fingolimod showed highest toxicity throughout treatment time. Cell death is low during the first 12 h period in all three drug conditions and cell viability is greater than 50%. The amount of cell death

has increased by 24 h. Compared to taxol, fingolimod has low cytotoxic effect on cancer cells. But when given in a combination with taxol, cell death is higher than the individual drugs. By the end of 48 h, cell viability is only 8% (92 % cell death) in the combination. This evidently indicated the synergistic effect of combination therapy worked more effectively when compared to individual drugs.

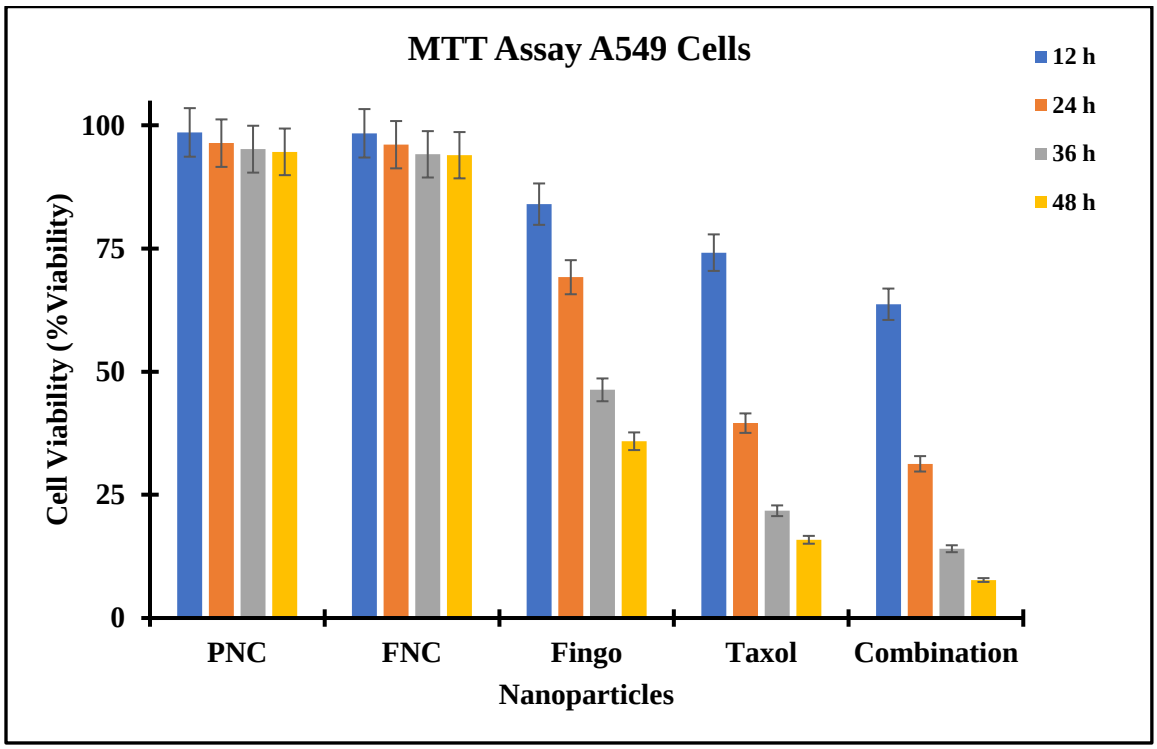

Figure 19. Time dependent cell viability assay in A549 cells with different nanoparticles. Lowest cell viability or highest cell death was observed in the combination treatment at 48 h. Cells without nanoparticle treatment were considered 100% viable.

MTT assay was also performed in VERO cells in the same manner as before. The VERO cell line lineage was isolated from kidney epithelial cells of the African green monkey. These cells were used for control study in this experiment. These cells do not possess folate receptors on their surface. As our nanomedicine is conjugated with folate, no cell death and very negligible cytotoxicity was observed **(Figure 20)**. This cytotoxicity experiment proved that the nanomedicine we synthesized is highly target specific and affects only cancer cells but not healthy cells.

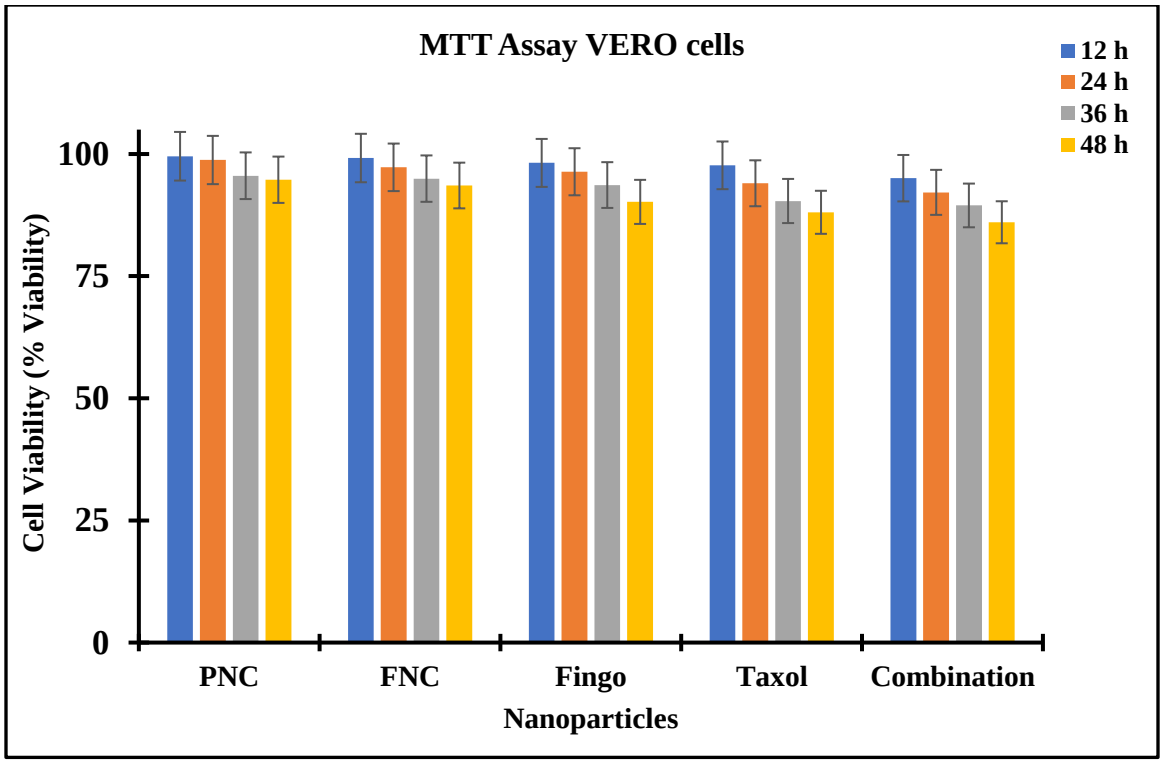

Figure 20. Time dependent cell viability assay in VERO cells with different nanoparticles. No cell death was observed because of the absence of folate receptors on surface of these cells.

2.3) Cellular internalization:

Fluorescence microscopic imaging study was done to evaluate the bioavailability, cellular internalization and therapeutic efficacy of functional nanoceria. From the previous works, we hypothesized that folate in the FNC is more likely to target the folate overexpressing receptors of tumor cells, which are lacked by normal cells. This results in the decrease of cytotoxicity to normal cells. For this study, lung cancer A549 cells and kidney epithelial Vero cells were incubated for 24 h and when they are enough confluent, PNC, FNC and functional FNC with only taxol drug and both drugs (taxol and fingolimod) were added to A549 cells and incubated for another 24 h. VERO cells were treated with FNC-Taxol-Fingo as a control for the study. When carboxylated nanoceria (**2,** PNC, **Figure 21, A-D**) encapsulated with DiI was incubated with the A549 cells, no internalization was observed. This is due to the lack of folic acid on the PAA coating of PNC. Tumor cells, when incubated with DiI encapsulated FNC (**3,** FNC,) for 24 h, show an effective internalization of nanoceria because of the folate groups. This was observed using the fluorescence microscopic images of the red color stained cytoplasm by DiI dye (**Figure 21, C-H**). To further study the treatment and internalization, theranostics encapsulated functional FNC was incubated with A549 cells for 24 h. After the incubation time, it was observed that the morphology of the

cells was changed as they were ruptured and killed (**Figure 21, I-P**). This confirms the internalization of the theranostics and an effective targeted drug delivery. No internalization or killing of VERO cells was observed by the nanomedicine (**Figure 21, Q-T**), since these cells lacks folate receptors and the nanomedicine specifically targets folate receptors. This confirms the targeted mechanism of our formulation.

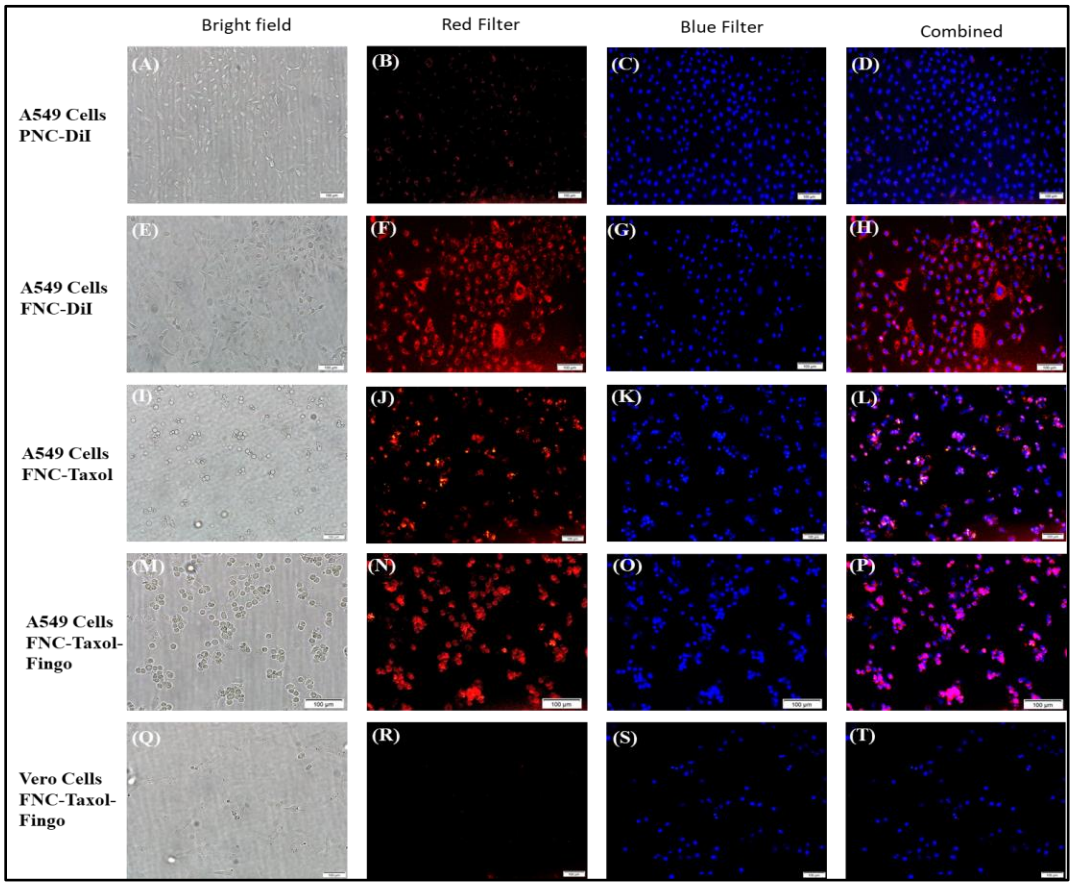

Figure 21. Images from fluorescence microscope showing (A-D) No or minimal internalization of carboxylic acid coated PNCs in the A549 cells due to the absence of folic acid. (E-F) Shows maximum internalization into the A549 cells without drugs, because of the presence of folic acid on the surface. (I-L) Effective killing of cells was observed with only taxol drug encapsulated in FNC. (M-P) Presence of both the drugs (taxol and fingolimod) leads to more cell death, compared to only taxol. (Q-T) No internalization in the normal kidney epithelial cells. Scale bar: 100 µm.

2.4) Intracellular Reactive oxygen species (ROS) Assay:

It is known that generation of ROS in the cells is an effective way for the treatment of cancer. Previous studies have shown the anti-tumor activity of taxol through ROS generation. We

hypothesized that when A549 cells are treated with drug loaded FNCs, they generate ROS and lead to cell death. To determine the amount of reactive oxygen species generated, dihydroethidium (DHE), a fluorescent dye was used. In presence of ROS, DHE oxidizes and forms 2-hydroethidium, which fluoresces red after intercalating within the nuclei. For the experiment, we cultured A549 cells in petri dishes, and when they are sufficiently confluent, these cells were treated with PNC, FNC and functional FNC with only taxol drug, FNC with both drugs (taxol and fingolimod). After incubating the cells with nanomedicine for 24h, we stained the cells with DHE dye for 30 min for the detection of ROS. Very minimal staining was observed in the A549 cells treated with PNC and FNC (**Figure 22, a-b)** because of very low stress. On the other hand, ROS levels are elevated in the cells treated with nanoparticles containing drugs (**Figure 22, c-d)**. Of these, FNC-Taxol-Fingo shows more ROS levels compared to FNC-Taxol, which further validates my hypothesis that there is a synergistic effect observed when treated with both drugs. This was further confirmed by histogram analysis of ROS using a commercially available software Image J. Through this software, we quantified the ROS generation using images obtained from fluorescence microscopy (**Figure 22, B)**. Taken together, these ROS experiments further indicated the effective function of nanoceria as drug carriers.

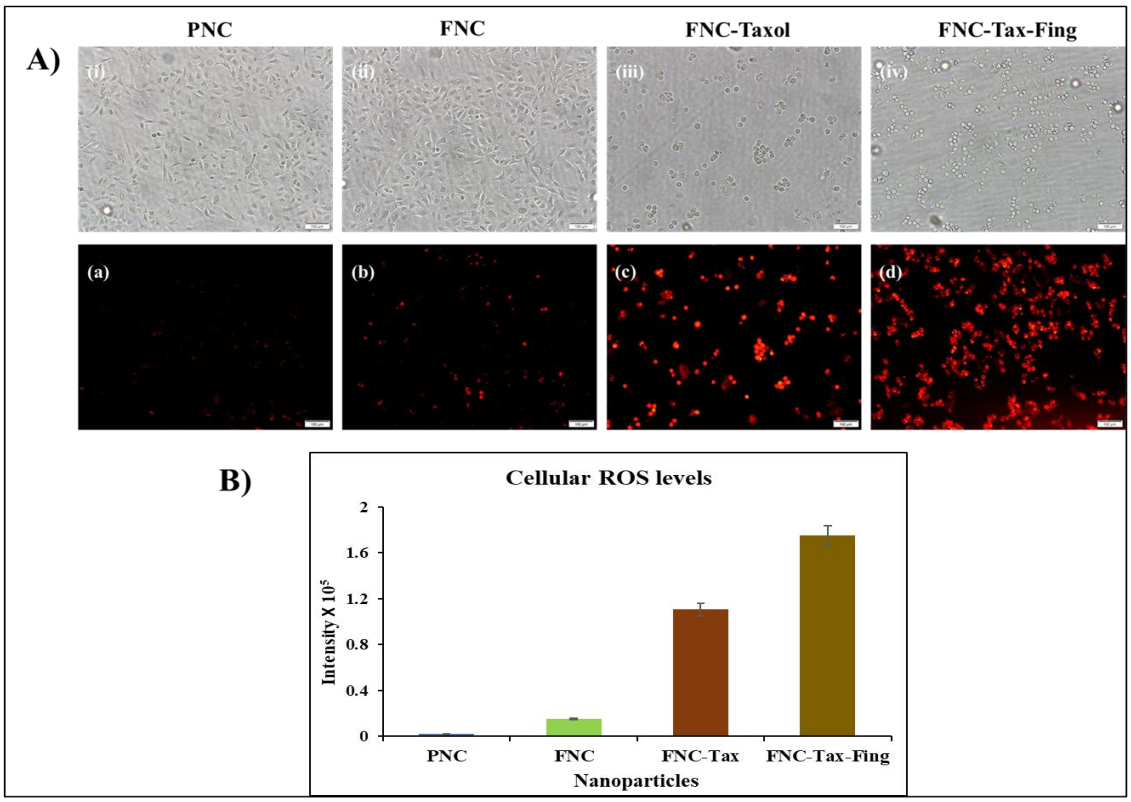

Figure 22. Determination and quantification of cytoplasmic ROS by NC **(A)** Fluorescence microscopic images of A549 cells **(a,b,c,d)** generating ROS in the presence of various functional

NC and **(i-iv)** respective bright field images. **(B)** ROS generation was quantified from the fluorescence images using Image J software. Scale bar: 100 µm.

2.5) Detection of Apoptotic and necrotic event:

After identifying ROS as the major mechanism for the cell death after drug treatment, we wanted to establish a connection between ROS generation and apoptotic cell death initiation. To investigate this, A549 cells were cultured in small petri dishes until they were 70% confluent and treated with PNC, FNC, FNC-taxol and FNC encapsulated with taxol and fingolimod (FNC-Taxol-Fingo, **Scheme 1**) for 24 h. For the detection of the cell death mechanism is either through apoptosis or necrosis pathway, fluorescence microscopic studies were done using dyes annexin V-FITC and ethidium homodimer III. Because of the absence of drugs, A549 cells treated with PNC and FNC are healthy and stable, hence minimal to no staining of cells was observed (**Figure 23, A-B)**. In contrast to this, a majority of the cells were stained with annexin V-FITC and exhibited green color fluorescence when treated with the drugs encapsulated nanoceria, which indicated the cell death is through apoptosis **(Figure 23, C-D)**. A very minimal number of cells had undergone necrosis and when stained with ethidium homodimer III, displayed a red color in the fluorescence imaging. This leads to the conclusion of this assay that both taxol and fingolimod had been leading the cancer cell death through apoptosis. Fluorescence imaging evidently suggests the drug delivering capabilities of nanoceria.

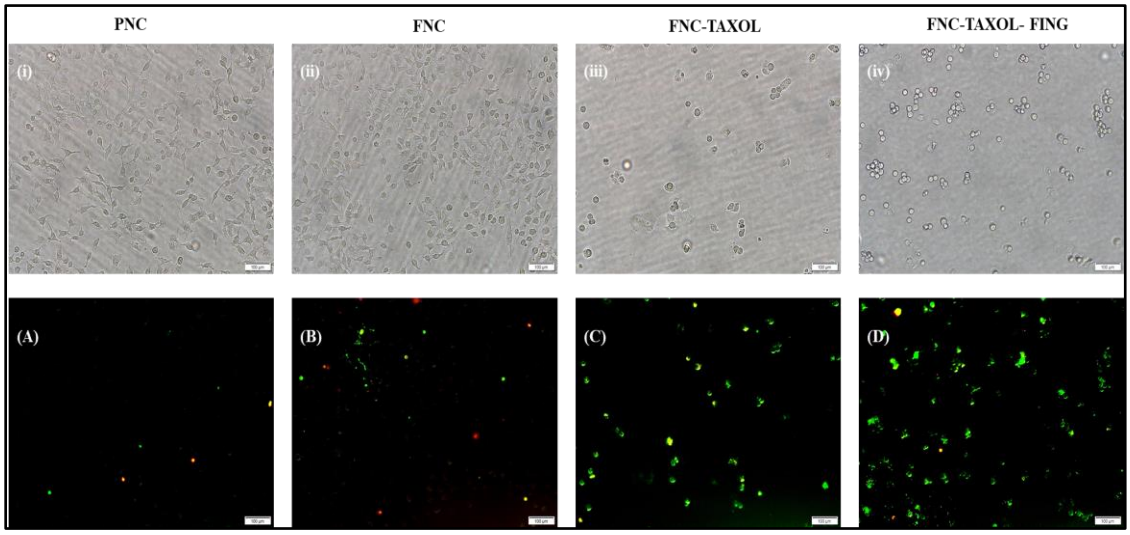

Figure 23. Detection of apoptotic cell death by fluorescence microscopy using annexin V-FITC and ethidium homodimer III. **(A)** and **(B)** Healthy cells emitted minimal fluorescence representing no cell death. **(C)** and **(D)** Apoptotic cells stained with FITC green fluorescence represents majority

of cell death occurred through apoptosis. Negligible cells gone through necrosis were stained with ethidium homodimer III emits and emitted red fluorescence. **i – iv** represents corresponding bright field images. Scale bar: 100 µm.

2.6) Migration assay:

The transwell migration assay has been performed to determine the anti-cancer properties of the nanomedicine we reported. A549 cells were seeded in the presence of serum free media for 24h in the invasion chamber of the migration plate. Once the cells were settled and attached to the bottom chamber, they were treated with PBS (control) and FNC loaded with taxol and fingolimod (FNC-Tax-Fing). Cells treated with the nanomedicine reported very few cells migrated to the feeder tray, whereas the control showed adequate cells had migrated to the feeder tray.**(Figure 24)**.

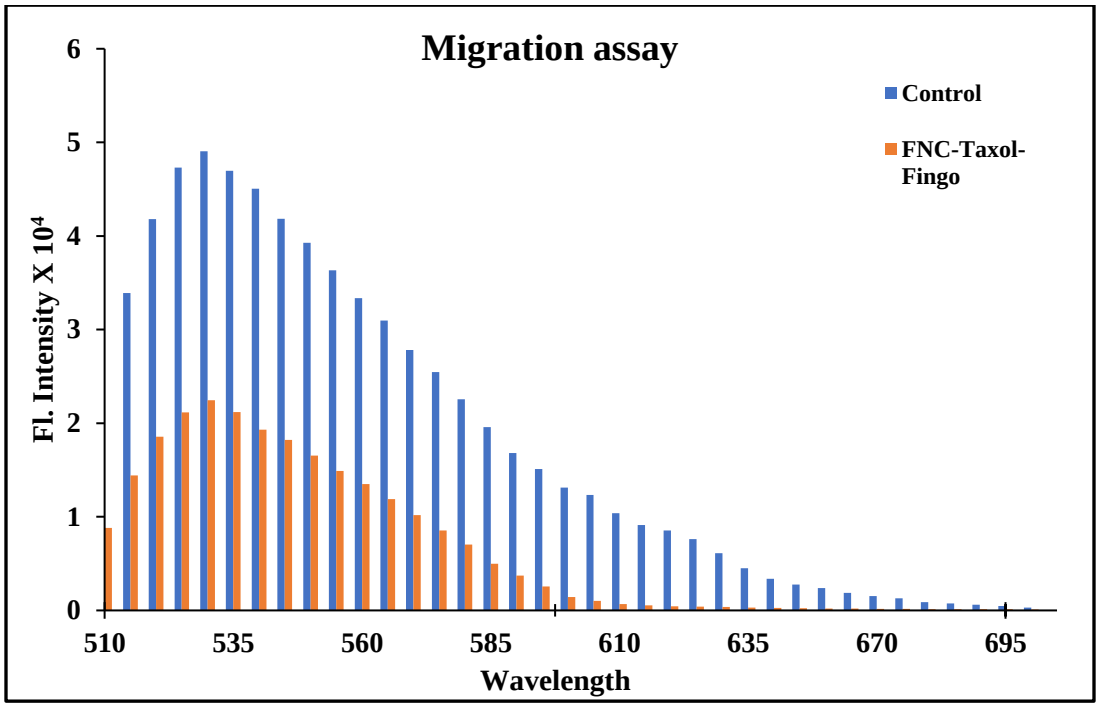

Figure 24. Migration assay showing the anti-metastatic property of FNC-Taxol-Fingo in A549 cells. Cells were treated with PBS as control and FNC-Taxol-Fingo.

Chapter III

Experimental Section

3.1) Materials:

Polyacrylic acid (PAA), 2-morpholinoethanesulfonic acid (MES), 1-ethyl-3-(3-(dimethylamino)-propyl carbodiimide hydrochloride (EDC), N,N′-dimethyl sulfoxide (DMSO), 3-(4,5-dimethylthiazol-2-yl)-2,5-diphenyltetrazolium bromide (MTT), chloropropyl amine, and N,N′-dimethylformamide (DMF) were purchased from Sigma-Aldrich and used as received. Near infrared DiI dye and 4,6-diamidino-2-phenylindole (DAPI) dye were purchased from Invitrogen. Cerium nitrate hexahydrate, N-hydroxy succinimide (NHS), tetrahydrofuran, acetonitrile, sodium azide, ammonium hydroxide, ethanol, folic acid, isopropanol, and MES sodium salt were purchased from ACROS organics and used without further purification. Dialysis membranes were received from spectrum laboratories. Dihydroethidium (DHE) was obtained from Cayman chemical, whereas H_2O_2 and paraformaldehyde were received from electron microscopy sciences. Fetal bovine serum (FBS) and 5X Annexin V binding buffer were purchased from BD Biosciences, whereas isopropyl alcohol, apoptosis and necrosis quantification kit (FITC-Annexin V, Ethidium homodimer III) were obtained from Biotium. Migration assay kit was purchased from Millipore. A549 cells (NSCLC), DMEM cell culture media were purchased from ATCC (U.S.A.).

3.2) Synthesis of Poly (acrylic acid) coated nanoceria (PNC):

PNC is synthesized using alkaline based precipitation method. For this synthesis, two solutions are required: 1) Poly (acrylic acid) (0.905 g) in 10 mL of DI water and 2) Cerium nitrate (0.901 g) in 2.5 mL DI water. Solution 2 was added to 30% ammonium hydroxide solution (30 mL), which was stirred at room temperature at high speed. After giving a 10-15 sec gap, solution 1 was added to the above mixture. Color change was observed on 10 min stirring from brown to dark brown. Then, the mixture was left on high stirring for 24 h and it turned to yellow color, which indicates the synthesis of stable nanoceria. This reaction was centrifuged three times, 20 min for each time at 3500, 4000 and 4500 rpm respectively, to reduce the size of PNC and to remove any aggregates formed. In the final step, this centrifuged PNC was subjected to dialysis for purification. This

process was conducted using the dialysis bag of molecular weight cutoff (MWCO) 6-8 K against the DI water and finally with phosphate buffer saline (PBS, pH = 7.4). The PNC obtained was stored at 4 ^{o}C for further characterizations **(1, Scheme 1)**.

3.3) Synthesis of Folate conjugated PNC with EDC-NHS chemistry:

At first, folic acid (10 mg) was mixed in 8 mL PBS (1X @7.4pH) in a 15 mL tube and mixed on a vortex machine till it became transparent. Then, 2 µL EDA (Ethylene Diamine) was mixed in 100 µL DMSO. Next, NHS (3 mg) was added to 100 µL of MES buffer (pH-6). Finally, before starting the reaction, EDC (5 mg) was added in 100 µL of MES buffer. This EDC mixture was added immediately to the folic acid solution in 2 parts 50 µL each time. Giving 15 sec gap, NHS solution was added to the mixture in same manner as EDC. After 3 min, EDA solution was added to the mixture 10 µL at 30 sec intervals with well mixing after each addition. This solution was placed on a tabletop mixture for 3 h.

2 solutions EDC and NHS were prepared for the surface conjugation. NHS (3 mg) was taken in 200 µL MES buffer. Then, 5 mg EDC was taken in 200 µL MES buffer. PNC (3 mL) which was already synthesized taken in a 15 mL tube. The EDC solution was added immediately after its synthesis to the PNC in 2 parts, 100 µL each time. After 15 sec, the NHS solution was added in 2 parts to the PNC solution. Finally, 300 µL folate-amine solution, which was synthesized earlier, added to PNC solution 5 µL each time at an interval of 30 sec and mixed well after each interval for better surface conjugation. Thus, we obtained folic acid conjugated nanoceria (FNC) . This was further characterized and used for the encapsulation of our cargo **(2, Scheme 1)**.

3.4) Encapsulation of DiI dye:

This process was done using solvent diffusion method. 2 mL of Nanoceria, both PNC and FNC were taken separately. To these, 1 mL PBS (@ 7.4 pH) was added and mixed. To this mixture, DiI dye (6 µL, 5 µg/mL dye in 100µL DMSO) was added dropwise with continuous stirring. Then, this mixture was dialyzed against PBS (@pH 7.4) for 2 h. In order to confirm this encapsulation successful, UV-vis and fluorescence spectrophotometric analysis was done.

3.5) Encapsulation of drugs:

This was also done by solvent diffusion method. 1 mL of PBS (7.4 pH) was mixed in 3 mL FNC. Then, DiI dye (2 µL, 5 µg/mL) and drugs taxol (20 µg/mL) and fingolimod (4 µL, 10 µg/mL) were mixed in 400 µL DMSO. This cargo mixture was added dropwise in the FNC with continuous stirring. This solution was dialyzed against PBS (7.4 pH) for 2 h. This functional nanoceria was ready for the cell culture experiments and stored at 4 ^{o}C for further studies.

3.6) Characterizations of Functional nanoceria:

Dynamic Light Scattering (DLS):

This was used to measure the size and surface charge of PNC, FNC and functional FNC. Machine used was Malvern's Nano-ZS90 zetasizer. The average size of PNC and FNC were 69.7 nm, 72.12 nm respectively and the zeta potentials were -46.1 and -29.3 mV **(Figure 15,16)**.

Spectrophotometric analysis:

UV-vis and fluorescence spectra of the FNC were recorded using the instrument TECAN's Infinite M200 PRO microplate reader and the samples were placed in the 96 well plate. Through this, the presence of folic acid, taxol and DiI dye in the FNC were determined by the values of absorbance and fluorescence obtained **(Figure 17,18)**.

Cell Studies:

3.7) Cytotoxicity studies using MTT assay:

This method was used to determine both time dependent and dose dependent cytotoxicity for the cell lines of lung cancer (A549). Experiment was conducted in a 96 well plate and each well was incorporated with approximately 2500 cells and treated with various functional nanoceria (2.0×10^{-3} mol) at 37 ^{o}C for different time points. After incubation time, each well was treated with MTT solution (5mM) and then incubated for 4-6 h, which results in the formation of formazan crystals (purple color). Acidic isopropanol (75 μL) was added to the crystals to dissolve and absorbance was recorded at 570 nm using TECAN microplate reader **(Figure 19,20)**.

3.8) Cell Internalization studies:

The A549 cells were taken in five small petri dishes and grown. When they were 75% confluent, treated with the following: Only PNC-COOH DiI, FNC-DiI, FNC-Tax-DiI and FNC-Tax-Fingo-DiI mix (2.0 mM) for 24 h in the humidified incubator (37 ^{o}C, 5% CO_2). After 24 h, these dishes were washed with 1x PBS (pH 7.4) and were fixed by adding 4% formaldehyde solution for 15 min. Then again washed with PBS and treated with 6-diamidino-2-phenylindole (DAPI, 5 mg/mL) dye for nuclei staining. Then cells were washed with PBS and images were taken using fluorescence microscope (Olympus IX73) **(Figure 21)**.

3.9) ROS Detection Assay:

A549 cells were seeded in 5 dishes and grown for 24 h. When they were 75% confluent, treated with PNC-COOH DiI, FNC-DiI, FNC-Tax-DiI and FNC-Tax-Fingo-DiI mix (2.0 mM) and incubated. After 24 h these were washed with 1x PBS and 20 μL of fluorescent DHE dye was added to each dish and incubated for 30 min at room temperature. Then these were washed with PBS and fixed using 4% formaldehyde for 15 min. Then washed with PBS and 2 mL PBS was added for storage. Optical images were taken using the fluorescence microscope (Olympus IX73) **(Figure 22)**.

3.10) Apoptosis and Necrosis assay:

This assay was carried out using Apoptosis and necrosis quantification kit obtained from Biotium. A549 cells were seeded in four dishes and treated with PNC-COOH DiI, FNC-DiI, FNC-Tax-DiI and FNC-Tax-Fingo-DiI mix (2.0 mM) and one dish was not treated. After incubating for 24 h, these were washed with 1x PBS and annexin-V-binding buffer (2 mL) was added to the dishes. Then 2 types of dyes- FITC annexin and ethidium dimer III (5 μL each) were added to the dishes and incubated for 15 min. Then washed with binding buffer and fixed with 4% formaldehyde 15 min. Later washed with binding buffer and binding buffer (2 mL) was added for storage and images were taken using fluorescence microscope (Olympus IX73) **(Figure 23, A)**. From the fluorescence images obtained, ROS fluorescence was quantified using commercial image J software. **(Figure 23, B)**

3.11) Migration assay:

The extent of migration showed by A549 cells has been determined using migration assay when they are treated with the drug combination and PBS as control. A Chemicon QCM 96-well cell migration assay kit from Millipore was used for the experiment. First, A549 cells were starved for 18-24 h in serum free media. Then, these cells (100 μL, 4000 cells) were seeded in top invasion chamber, which contains collagen layer. Following this step, seeded cells were treated with nanomedicine (FNC-Tax-Fingo, 30 μL, 2.0 mM) and PBS (Control). After seeding and inoculation, invasion chamber was placed on the feeder tray consisting of media with 10% serum. This assembly was placed in an incubator at 37 ^{o}C for 24 h. This provides a window period for starved A549 cells to invade the collagen layer. These migrated cells trapped in the collagen layer were detached by incubating them on feeder tray containing cell detachment buffer (100 μL) for 1 h. Detached cells were stained with CyQuant dye and fluorescence was recorded using TECAN infinite M200 PRO microplate reader at λ_{em} = 520 nm. (**Figure 24**)

Chapter IV

Conclusion and Future Study

FNC-Taxol-Fingo nanoparticles were successfully synthesized for the treatment of A549 lung cancer cells by conjugating folic acid on cerium oxide nanoparticles and encapsulating drugs taxol and fingolimod. Folic acid on the surface helps nanomedicine to achieve target specificity, since cancer A549 cells shows high folate reception. Combination of both the drugs were encapsulated to give synergistic effect. Cytotoxicity of the nanomedicine was assessed using cell based assay. Synergistic effect of the drugs was confirmed by conducting apoptosis experiments. Anti-metastatic property of the drugs was confirmed through migration assay. Through these experiments, we concluded that drugs encapsulated nanoceria proved to be an ideal vehicle for drug delivery and combination was a successful model for treatment of cancer.

In the future, we are planning to duplicate and triplicate this study for more accurate and effective results. We are planning to add more experiments for this study like scratch assay. For better understanding of these properties, in vivo studies will be done in the future. Hence, this research will help in the progression for more effective treatment of cancer.

References

1. American Cancer Society. *Cancer Facts and Figures* **2019**, Atlanta, GA.
2. https://www.who.int/news-room/fact-sheets/detail/cancer
3. Sung, H.; Ferlay, J.; Bray, F.; Global cancer statistics 2020: GLOBOCAN estimates of incidence and mortality worldwide for 36 cancers in 185 countries. *CA: A cancer general for clinicians* **2020**
4. Jemal, A.; Center, M. M.; DeSantis, C.; Ward, E. M. Global patterns of cancer incidence and mortality rates and trends. *Cancer Epidemiol. Biomarkers Prev*. **2010**, 19, 1893−1907.
5. Youlden, D. R.; Cramb, S. M.; Baade, P. D. The International Epidemiology of Lung Cancer: Geographical Distribution and Secular Trends. *Journal of Thoracic Oncology* **2008**, 3, 819–831
6. Proia, D. A.; Sang, J.; He, S.; Smith, D. L.; Sequeira, M.; Zhang, C.; Liu, Y.; Ye, S.; Zhou, D.; Blackman, R. K.; Foley, K. P.; Koya. K.; Wada, Y. Synergistic activity of the Hsp90 inhibitor ganetespib with taxanes in non-small cell lung cancer models. *Investigational New Drugs* **2012**, 30, 2201-2209.
7. Chabner, B. A.; Roberts, G. T. Chemotherapy and the war on cancer. *Nat. Rev. Cancer*, **2005**, 5, 65–72.
8. Acquaviva, J.; Smith, D. L.; Sang, J.; Friedland, J. C.; He, S.; Sequeira, M.; Zhang, C.; Wada, Y.; Proia, D. A. Targeting KRAS mutant non-small cell lung cancer with the Hsp90 inhibitor ganetespib. *Mol. Cancer Ther*. **2012**, 11, 2633−2643.
9. Couraud, S.; Zalcman, G.; Milleron, B.; Morin, F.; & Souquet, P. J. Lung cancer in never smokers-A review. *European Journal of Cancer* **2012**, 48, 1299–1311.
10. Soria, J. C.; Lee, H. Y.; Lee, J. I.; Wang, L.; Issa, J. P.; Kemp, B. L.; Liu, D. D.; Kurie, J. M.; Mao, L.; Khuri, F. R. Lack of PTEN Expression in Non-Small Cell Lung Cancer Could Be Related to Promoter Methylation. *Clin. Cancer Res*. **2002**, 8, 1178–1184.
11. Sundarraj, S.; Thangam, R.; Sujitha, M. V.; Vimala, K.; Kannan, S. Ligand-conjugated mesoporous silica nanorattles based on enzyme targeted prodrug delivery system for effective lung cancer therapy. *Toxicol. Appl. Pharmacol*. **2014**, 275(3): 232–243.
12. Schiller, J. H.; Harrington, D.; Belani, C. P.; Langer, C.; Sandler, A.; Krook, J. Comparison of four chemotherapy regimens for advanced non- small-cell lung cancer. *N Engl J Med* **2002**, 346, 92–8.
13. Schabath, B. M.; Cote, M. L. Cancer progress and priorities: Lung cancer. *Cancer epidemiology, biomarkers and prevention* **2019**

14. Collins, L. G.; Haines, C.; Perkel, R.; Enck, R. E. Lung cancer: diagnosis and management. *American family physician* **2007**, 75(1), 56–63.
15. McLean, A.; Barnes, D. J.; Troy, L. K. Diagnosing Lung Cancer: The Complexities of Obtaining a Tissue Diagnosis in the Era of Minimally Invasive and Personalized Medicine. *Journal of clinical medicine* **2018**, 7(7), 163.
16. Omura, K. Current status of oral cancer treatment strategies: surgical treatments for oral squamous cell carcinoma. *Int J Clin Oncol* **2014**, 19, 423–430.
17. Demaria, S.; Golden, E. B.; Formenti, S. C. Role of Local Radiation Therapy in Cancer Immunotherapy. *JAMA Oncol.* **2015**, 1(9):1325–1332.
18. Mellor, H. R.; Callaghan, R. Resistance to Chemotherapy in Cancer: A Complex and Integrated Cellular Response. *Pharmacology* **2008**, 81(4), 275–300.
19. Demaria, M.; O'Leary, M. N.; Chang, J.; Shao, L.; Liu, S. Cellular Senescence Promotes Adverse Effects of Chemotherapy and Cancer Relapse. *Cancer Discovery* **2016**, 7(2), 165–176.
20. Sanoff, H. K.; Deal, A. M.; Krishnamurthy, J.; Sorrentino, J. Effect of cytotoxic chemotherapy on markers of molecular age in patients with breast cancer. *J Natl Cancer Inst.* **2014**,106.
21. Pang, B.; Qiao, X.; Janssen, L.; Kerkhoven, R. Drug-induced histone eviction from open chromatin contributes to the chemotherapeutic effects of doxorubicin. *Nat Commun*. **2013**, 4, 1908.
22. Van Vlerken, L. E.; Amiji, M. Multi-functional polymeric nanoparticles for tumor-targeted drug delivery. *Expert Opin. Drug Delivery* **2006**, 3, 205−216.
23. Hong, Y.; Che, S.; Hui, B.; Yang, Y.; Wang, X.; Zhang, H. Lung cancer therapy using doxorubicin and curcumin combination: Targeted prodrug based, pH sensitive nanomedicine. *Biomedicine and Pharmacotherapy* **2015**, 112.
24. Ma, X.; Huang, X.; Moore, Z.; Huang, G.; Kilgore, J. A.; Wang, Y.; Gao, J. Esterase-activatable β-lapachone prodrug micelles for NQO1-targeted lung cancer therapy. *Journal of Controlled Release* **2009**, 7, 201–211.
25. Singh, S. Nanomedicine-nanoscale drugs and delivery systems. *J. Nanosci. Nanotechnol*. **2010**, 10, 7906−7918.
26. Van der Meel, R.; Sulheim, E.; Shi, Y. Smart cancer nanomedicine. *Nat. Nanotechnol*. **2014**, 3, 1007–1017.

27. Hu, F.; Macrenaris, K. W.; Waters, A.; Schultz-Sikma, E. A.; Eckermann, A. L.; Meade, T. J. Highly dispersible, superparamagnetic magnetite nanoflowers for magnetic resonance imaging. *Chem. Commun*. **2010**, 46, 73–75.
28. McCarthy, J. R.; Perez, J. M.; Brückner, C.; Weissleder, R. Polymeric nanoparticle preparation that eradicates tumors. *Nano Lett*. **2005**, 5, 2552-2556.
29. Babu, A.; Templeton, A. K.; Munshi, A.; Ramesh, R. Nanoparticle-based drug delivery for therapy of lung cancer: Progress and challenges. *Nanomater*. **2013**, 5, 1-11.
30. Sukumar, U. K.; Bhushan, B.; Dubey, P.; Matai, I.; Sachdev, A.; Packirisamy, G. Emerging applications of nanoparticles for lung cancer diagnosis and therapy. *Int. Nano Lett*. **2013**, 3, 117.
31. Soppimath, K. S.; Aminabhavi, T. M.; Kulkarni, A. R.; Rudzinski, W. E. Biodegradable polymeric nanoparticles as drug delivery devices. *Journal of Controlled Release* **2001**, 70, 1–20.
32. Wang, Y.; Grayson, S. M. Approaches for the preparation of non-linear amphiphilic polymers and their applications to drug delivery. *Adv. Drug Delivery Rev*. **2012**, 64, 852–865.
33. Kainthan, R. K.; Brooks, D. E. Unimolecular micelles based on hydrophobically derivatized hyperbranched polyglycerols: Biodistribution studies. *Bioconjugate Chem*. **2008**, 19, 2231–2238.
34. Stiriba, S.; Frey, H.; Haag, R.; Angew, B. Dendritic polymers in biomedical applications: From potential to clinical use in diagnostics and therapy. *Chem. Int. Ed.* **2002**, 41, 1329–1334.
35. Stumbé, J.; and Bruchmann, B. Hyperbranched polyesters based on adipic acid and glycerol. Macromol. *Rapid Commun*. **2004**, 25, 921–924.
36. Acharya, S.; Sahoo, S. K. PLGA nanoparticles containing various anticancer agents and tumor delivery by EPR effect. *Advanced Drug Delivery Reviews* **2011,** 63(3), 170–183.
37. Gupta, H.; Aqil, M.; Khar, R. K.; Ali, A., Bhatnagar, A.; Mittal, G. Sparfloxacin-loaded PLGA nanoparticles for sustained ocular drug delivery. *Nanomedicine: Nanotechnology, Biology and Medicine* **2010,** 6(2), 324–333.
38. Buhecha, M. D.; Lansley, A. B.; Somavarapu, S.; Pannala, A. S. Development and characterization of PLA nanoparticles for pulmonary drug delivery: Co-encapsulation of theophylline and budesonide, a hydrophilic and lipophilic drug. *Journal of Drug Delivery Science and Technology* **2019,** 53, 101128.

39. Ahmad, Z.; Shah, A.; Siddiq, M.; Kraatz, H. B. Polymeric micelles as drug delivery vehicles. *RSC Adv*. **2014**, 4(33), 17028–17038.
40. Kedar, U.; Phutane, P.; Shidhaye, S.; Kadam, V. Advances in polymeric micelles for drug delivery and tumor targeting. *Nanomedicine: Nanotechnology, Biology and Medicine* **2010**, 6(6), 714–729.
41. Matsumura, Y.; Kataoka, K. Preclinical and clinical studies of anticancer agent-incorporating polymer micelles. *Cancer Science* **2009**, 100(4), 572–579.
42. Makhmalzade, B. S.; Chavoshy, F. Polymeric micelles as cutaneous drug delivery system in normal skin and dermatological disorders. *J Adv Pharm Technol Res.* **2018**, 9:2-8.
43. Liu, J.; Li, H. J.; Luo, Y. L.; Chen, Y. F.; Fan, Y. N.; Du, J. Z.; Wang, J. Programmable delivery of immune adjuvant to tumor-infiltrating dendritic cells for cancer immunotherapy. *Nano Letters* **2020**, 20, 4882–4889.
44. Santra, S.; Kaittanis, C.; Perez, J. M. Aliphatic hyperbranched polyester: A new building block in the construction of multifunctional nanoparticles and nanocomposites. *Langmuir* **2010**, 26, 5364–5373.
45. Santra, S.; Kaittanis, C.; Perez, J. M. Cytochrome c encapsulating theranostic nanoparticles: A novel bifunctional system for targeted delivery of therapeutic membrane-impermeable proteins to tumors and imaging of cancer therapy. *Mol. Pharmaceutics* **2010**, 7, 1209−1222.
46. Hutnick, M. A.; Ahsanuddin, S.; Guan, L.; Lam, M.; Baron, E. D.; Pokorski, J. K. PEGylated Dendrimers as Drug Delivery Vehicles for the Photosensitizer Silicon Phthalocyanine Pc 4 for Candidal Infections. *Biomacromolecules* **2017**, 18(2), 379–385.
47. Shaw, Z.; Patel, A.; Butcher, T.; Banerjee, T.; Bean, R.; Santra, S. Pseudo-branched polyester copolymer: an efficient drug delivery system to treat cancer. *Biomater. Sci*. **2020**, 8, 1481-1772.
48. Laquintana, V.; Denora, N.; Lopalco, A.; Lopedota, A.; Cutrignelli, A.; Lasorsa, F. M.; Agostino, G.; Franco, M. Synthesis, characterization, and in Vitro evaluation of a new TSPO-selective bifunctional chelate ligand. *Mol. Pharmaceutics* **2014**, 11, 859–871.
49. Lin, W.; Huang, Y. W.; Zhou, X. D.; Ma, Y. The toxicity of nanoparticles depends on multiple molecular and physicochemical mechanisms. *Int. J Toxicol.* **2006**, 25, 51−457.
50. Ocsoy, I.; Tasdemir, D.; Mazicioglu, S.; Celik, C.; Kati, A.; Ulgen, F. Biomolecules incorporated metallic nanoparticles synthesis and their biomedical applications. *Materials Letters* **2017**, 212, 45-50.

51. Tan, W. B.; Huang, N.; Zhang, Y. Biocompatible fluorescent core-shell nanoconjugates based on chitosan/Bi2S3 quantum dots. *Journal of Colloid and Interface Science* **2017**, 310, 464–470.
52. Uzgiris, E.E.; Cline, H.; Moasser, B.; Grimmond, B.; Amaratunga, M.; Smith, J.F.; Goddard, G. Contrast agents for magnetic resonance imaging synthesized with ring-opening metathesis polymerization. *Biomacromolecules* **2004**, 5, 54–61.
53. Josephson, L.; Tung, C. H.; Moore, A.; Weissleder, R. High-efficiency intracellular magnetic labeling with novel superparamagnetic-tat peptide conjugates. *Bioconjugate Chem*. **1999**, 10, 186–191.
54. Chertok, B.; Moffat, B. A.; David, A. E.; Yu, F.; Bergemann, C.; Ross, B. D.; Yang, V. C. Iron oxide nanoparticles as a drug delivery vehicle for MRI monitored magnetic targeting of brain tumors. *Biomaterials* **2008**, 29(4), 487–496.
55. Banerjee, T.; Tummala, T.; Elliott, R., Jain, V., Brantley, W.; Hadorn, L.; Santra, S. Multimodal Magneto-Fluorescent Nanosensor for Rapid and Specific Detection of Blood-Borne Pathogens. *ACS Applied Nano Materials* **2019**, 2, 5587-5593.
56. Giljohann, D. A.; Seferos, D. S.; Daniel, W. L.; Massich, M. D.; Patel, P. C.; Mirkin, C. A. Gold Nanoparticles for Biology and Medicine. *Angewandte Chemie International Edition* **2010**, 49(19), 3280–3294.
57. Huang, X.; Jain, P. K.; El-Sayed, I. H.; El-Sayed, M. A. Gold nanoparticles: interesting optical properties and recent applications in cancer diagnostics and therapy. *Nanomedicine* **2007**, 2(5), 681–693.
58. Cheng, J.; Gu, Y.-J.; Cheng, S. H.; Wong, W.T. Surface Functionalized Gold Nanoparticles for Drug Delivery. *Journal of Biomedical Nanotechnology* **2013**, 9(8), 1362–1369.
59. Peng, G.; Tisch, U.; Adams, O.; Hakim, M.; Shehada, N.; Broza, Y. Y.; Haick, H. Diagnosing lung cancer in exhaled breath using gold nanoparticles. *Nature Nanotechnology* **2009**, 4(10), 669–673.
60. Huang, X.; El-Sayed, M. A. Gold nanoparticles: Optical properties and implementations in cancer diagnosis and photothermal therapy. *Journal of Advanced Research* **2010**, 1(1), 13–28.
61. Nishimori, H.; Kondoh, M.; Isoda, K.; Tsunoda, S.; Tsutsumi, Y.; Yagi, K. Silica nanoparticles as hepatotoxicants. *European Journal of Pharmaceutics and Biopharmaceutics* **2009**, 72(3), 496–501.

62. Lu, J.; Liong, M.; Li, Z.; Zink, J. I.; Tamanoi, F. Biocompatibility, Biodistribution, and Drug-Delivery Efficiency of Mesoporous Silica Nanoparticles for Cancer Therapy in Animals. *Small***. 2010**, 6(16), 1794–1805.
63. Zhang, Q.; Liu, F.; Nguyen, K. T.; Ma, X.; Wang, X.; Xing, B.; Zhao, Y. Multifunctional Mesoporous Silica Nanoparticles for Cancer-Targeted and Controlled Drug Delivery. *Advanced Functional Materials* **2012**, 22(24), 5144–5156.
64. Ohulchanskyy, T. Y.; Roy, I.; Goswami, L. N.; Chen, Y.; Bergey, E. J.; Pandey, R. K.; Prasad, P. N. Organically Modified Silica Nanoparticles with Covalently Incorporated Photosensitizer for Photodynamic Therapy of Cancer. *Nano Letters* **2007**, 7(9), 2835–2842.
65. Hudson, S.P.; Padera, R.F.; Langer, R.; Kohane, D.S. *Biomaterials* **2008**, 29, 4045–4055.
66. Dos Santos, C. A.; Seckler, M. M.; Ingle, A. P.; Gupta, I.; Galdiero, S.; Galdiero, M.; Rai, M. Silver Nanoparticles: Therapeutical Uses, Toxicity, and Safety Issues. *Journal of Pharmaceutical Sciences* **2014**, 103(7), 1931–1944.
67. Foldbjerg, R.; Dang, D. A.; Autrup, H. Cytotoxicity and genotoxicity of silver nanoparticles in the human lung cancer cell line, A549. *Archives of Toxicology* **2010**, 85(7), 743–750.
68. Kumar, C. G.; Poornachandra, Y. Biodirected synthesis of Miconazole-conjugated bacterial silver nanoparticles and their application as antifungal agents and drug delivery vehicles. Colloids and Surfaces *B: Biointerfaces* **2015**, 125, 110–119.
69. Yuan, Y. G.; Peng, Q. L.; Gurunathan, S. Silver nanoparticles enhance the apoptotic potential of gemcitabine in human ovarian cancer cells: combination therapy for effective cancer treatment. *International Journal of Nanomedicine* **2017**, 12, 6487–6502.
70. Liu, B.; Sun, Z.; Huang, P. J.; Liu, J. Hydrogen Peroxide Displacing DNA from Nanoceria: Mechanism and Detection of Glucose in Serum. *Journal of the American Chemical Society* **2015**, 137(3), 1290–1295.
71. Tarnuzzer, R. W.; Colon, J.; Patil, S.; Seal, S. Vacancy engineered ceria nanostructures for protection from radiation-induced cellular damage. *Nano Lett*. **2005**, 5, 2573−2577.
72. Pirmohamed, T.; Dowding, J. M.; Singh, S.; Wasserman, B.; Heckert, E.; Karakoti, A. S.; Self, W. T. Nanoceria exhibit redox state-dependent catalase mimetic activity. *Chemical Communications* **2010**, 46(16), 2736.
73. Kumar, A.; Das, S.; Munusamy, P.; Self, W.; Baer, D. R.; Sayle, D. C.; Seal, S. Behavior of nanoceria in biologically-relevant environments. *Environ. Sci.: Nano* **2014**, 1(6), 516–532.

74. Maia, J.; Ferreira, L.; Carvalho, R.; Ramos, M. A.; Gil, M. H. Synthesis and characterization of new injectable and degradable dextran-based hydrogels. *Polymer* **2005**, 46(23), 9604–9614.
75. Chen, J.; Patil, S.; Seal, S.; McGinnis, J. F. Rare earth nanoparticles prevent retinal degeneration induced by intracellular peroxides. *Nature Nanotechnology* **2006**, 1(2), 142–150.
76. Patel, P.; Kansara, K.; Singh, R.; Shukla, R. K.; Singh, S.; Dhawan, A.; Kumar, A. Cellular internalization and antioxidant activity of cerium oxide nanoparticles in human monocytic leukemia cells. *International Journal of Nanomedicine* **2018**, 13, 39–41.
77. Korsvik, C.; Patil, S.; Seal, S.; Self, W. T. Superoxide dismutase mimetic properties exhibited by vacancy engineered ceria nanoparticles. Chemical Communications **2007**, (10), 1056.
78. Zal, Z.; Ghasemi, A.; Azizi, S.; Omran, H.; Montazeri, A.; Hosseinimehr, S. J. Radioprotective Effect of Cerium Oxide Nanoparticles Against Genotoxicity Induced by Ionizing Radiation on Human Lymphocytes. *Current radiopharmaceuticals* **2018**, 11(2), 109–115.
79. Panda, S. R.; Singh, R. K.; Priyadarshini, B.; Rath, P. P.; Parhi, P. K.; Sahoo, T. R. Nanoceria: A rare-earth nanoparticle as a promising anti-cancer therapeutic agent in colon cancer. *Materials Science in Semiconductor Processing* **2019**, 104, 104669.
80. Diaconeasa, Z.; Barbu, L.; Coman, C.; Leopold, L.; Mesaros, A.; Pop, O.; Rugina, D.; Stefan, R.; Socaciu, C. Cerium Oxide Nanoparticles and Its Cytotoxicity Human Lung Cancer Cells. *Romanian Biotechnological Letters* **2015**, 20(4), 10679-10687.
81. Corsi, F.; Caputo, F.; Traversa, E.; Ghibelli, L. Not Only Redox: The Multifaceted Activity of Cerium Oxide Nanoparticles in Cancer Prevention and Therapy. *Frontiers in Oncology* **2018**, 8.
82. Popova, N. R.; Popov, A. L.; Ermakov, A. M.; Reukov, V. V.; Ivanov, V. K. Ceria-Containing Hybrid Multilayered Microcapsules for Enhanced Cellular Internalization with High Radioprotection Efficiency. *Molecules* **2020**, 25(13), 2957.
83. Allen, M. J.; MacRenaris, K. W.; Venkatasubramanian, P. N.; Meade, T. J. Cell-permeable MR contrast agents with increased intracellular retention. *Chem. Biol.* **2004**, 11, 301–307.
84. Alemzadeh, E.; Dehshahri, A.; Izadpanah, K.; Ahmadi, F. Plant virus nanoparticles: Novel and robust nanocarriers for drug delivery and imaging. *Colloids and Surfaces B: Biointerfaces* **2018**, 167, 20–27.

85. Zhang, R. X.; Wong, H. L.; Xue, H. Y.; Eoh, J. Y.; Wu, X. Y. Nanomedicine of synergistic drug combinations for cancer therapy – Strategies and perspectives. *Journal of Controlled Release* **2013**, 240, 489–503.
86. Lin, H.; Hu, B.; He, X.; Mao, J.; Wang, Y.; Wang, J.; Zhang, F. Overcoming taxol-resistance in A549 cells: A comprehensive strategy of targeting P-gp transporter, AKT/ERK pathways, and cytochrome P450 enzyme CYP1B1 by 4-hydroxyemodin. *Biochemical Pharmacology* **2019**, 9, 246-258
87. Alshaker, H.; Wang, Q.; Srivats, S.; Chao, Y.; Cooper, C.; Pchejetski, D. New FTY720-docetaxel nanoparticle therapy overcomes FTY720-induced lymphopenia and inhibits metastatic breast tumor growth. *Breast Cancer Res. Treat.* **2017**, 165, 531–543.
88. Li, Y.; Hu, T.; Chen, T.; Yang, T.; Ren, H.; Chen, M. Combination treatment of FTY720 and cisplatin exhibits enhanced antitumor effects on cisplatin-resistant non-small lung cancer cells. *Oncology reports* **2018**, 39, 565-572.